SEMANTIC SCENE CLASSIFICATION FOR CONTENT-BASED IMAGE RETRIEVAL

A THESIS
SUBMITTED TO THE DEPARTMENT OF COMPUTER ENGINEERING
AND THE INSTITUTE OF ENGINEERING AND SCIENCE
OF BILKENT UNIVERSITY
IN PARTIAL FULFILLMENT OF THE REQUIREMENTS
FOR THE DEGREE OF
MASTER OF SCIENCE

By
Özge Çavuş

August, 2008

I certify that I have read this thesis and that in my opinion it is fully adequate, in scope and in quality, as a thesis for the degree of Master of Science.

Asst. Prof. Dr. Selim Aksoy(Advisor)

I certify that I have read this thesis and that in my opinion it is fully adequate, in scope and in quality, as a thesis for the degree of Master of Science.

Prof. Dr. Gözde Bozdağı Akar

I certify that I have read this thesis and that in my opinion it is fully adequate, in scope and in quality, as a thesis for the degree of Master of Science.

Asst. Prof. Dr. Pınar Duygulu Şahin

Approved for the Institute of Engineering and Science:

Prof. Dr. Mehmet B. Baray
Director of the Institute

ABSTRACT

SEMANTIC SCENE CLASSIFICATION FOR CONTENT-BASED IMAGE RETRIEVAL

Özge Çavuş
M.S. in Computer Engineering
Supervisor: Asst. Prof. Dr. Selim Aksoy
August, 2008

Content-based image indexing and retrieval have become important research problems with the use of large databases in a wide range of areas. Because of the constantly increasing complexity of the image content, low-level features are no longer sufficient for image content representation. In this study, a content-based image retrieval framework that is based on scene classification for image indexing is proposed. First, the images are segmented into regions by using their color and line structure information. By using the line structures of the images the regions that do not consist of uniform colors such as man made structures are captured. After all regions are clustered, each image is represented with the histogram of the region types it contains. Both multi-class and one-class classification models are used with these histograms to obtain the probability of observing different semantic classes in each image. Since a single class with the highest probability is not sufficient to model image content in an unconstrained data set with a large number of semantically overlapping classes, the obtained probability values are used as a new representation of the images and retrieval is performed on these new representations. In order to minimize the semantic gap, a relevance feedback approach that is based on the support vector data description is also incorporated. Experiments are performed on both Corel and TRECVID datasets and successful results are obtained.

Keywords: content based image retrieval, relevance feedback, scene classification, segmentation.

ÖZET

İÇERİK TABANLI GÖRÜNTÜ ERİŞİMİ İÇİN ANLAMSAL SAHNE SINIFLANDIRMASI

Özge Çavuş
Bilgisayar Mühendisliği, Yüksek Lisans
Tez Yöneticisi: Yard. Doç. Dr. Selim Aksoy
Ağustos, 2008

Son yıllarda çok geniş veri tabanlarının kullanımıyla birlikte içerik tabanlı görüntü indekslemesi ve erişimi önemli bir araştırma konusu halini almıştır. Görütü indekslenmesinde kullanılan alt düzey öznitelikler görüntülerin karmaşık içeriklerini yeterli olarak ifade edememektedirler. Bu çalışmada, görüntü indekslemesi için sahne sınıflandırmasını baz alan bir görüntü erişim sistemi tanımlanmıştır. İlk olarak renk ve doğrusal çizgi yapı özellikleri kullanılarak görüntüler bölütlenmiştir. Çizgi yapı özellikleri kullanılarak, insan yapısı gibi birörnek renklerden oluşmayan yapıların görüntülerden bölütlenmesi hedeflenmektedir. Bölütleme sonucunda elde edilen tüm bölütler k-means öbekleme algoritması kullanılarak öbeklendikten sonra, her görüntü içermiş olduğu bölüt türlerinin histogramıyla ifade edilmiştir. Elde edilen histogramlar üzerinde çok sınıflı ve tek sınıflı sınıflandırıcılar eğitilmiş ve her görüntü için o görüntünün farklı sınıflara ait olma olasılıkları bulunmuştur. Bir görüntü aynı anda birden fazla sınıfa ait olabileceğinden, görüntüleri en yüksek olasılık değerini veren sınıfla etiketlemek yeterli olmayabilir. Bu nedenle, görüntüler tüm sınıflara ait olma olasılıkları ile indekslenmiş ve içerik tabanlı görüntü erişimi bu indeksler kullanılarak gerçekleştirilmiştir. Görüntü erişim sistemini insan algısıyla desteklemek ve anlambilimsel uçurumu en aza indirgemek için erişim senaryosuna tek sınıf sınıflandırıcı bazlı ilgililik geri beslemesi eklenmiştir. Bunun için, ilgili görüntüleri çok iyi modelleyen, ilgili olmayan görüntülerden de bir o kadar uzak duran bir hiperküre oluşturan destek vektör veri tanımlaması kullanılmıştır. Önerilen yöntemler TRECVID ve Corel veri kümelerinde denenmiş ve başarılı sonuçlar elde edilmiştir.

Anahtar sözcükler: içerik tabanlı görüntü erişimi, ilgililik geri beslemesi, sahne sınıflandırması, bölütleme.

Acknowledgement

I would like to express my sincere gratitude to my supervisor Asst. Prof. Dr. Selim Aksoy for his instructive comments, suggestions, support and encouragement during this thesis work.

I am grateful to Prof. Dr. Gözde Bozdağı Akar and Asst. Prof. Dr. Pınar Duygulu Şahin for reading and reviewing this thesis.

This work was supported in part by the TÜBİTAK Grant 104E077.

Contents

List of Figures

List of Tables

Chapter 1

INTRODUCTION

1.1 Motivation

Content based image indexing and retrieval (CBIR) has become an extremely important issue with the use of large databases in a wide range of areas. Searching in huge image datasets according to their contents has been the major subject of many research areas in the last decade. Many studies are proposed for content-based analysis, indexing and retrieval in these types of datasets [11, 38, 4, 36, 34, 33, 27].

In CBIR, the image contents are represented by low-level features that are extracted from the images automatically by using several low-level feature extraction algorithms. Most of early approaches have resorted to global feature extraction to represent the images [13, 30, 9, 7, 31, 34, 33]. However the global features can not catch the semantic content of the images that humans receive. Hence the results of retrieval process may not satisfy the user.

In order to solve this problem, recent works propose techniques that uses local descriptors [10, 27] instead of global ones while indexing the images and include local information of the images in the model. Although these types of techniques have more advantages compared to global based ones, they are not successful enough to model the visual content of the images.

The contextual information is very important to reflect the semantic content of the images. Having knowledge about the contextual information provides contribution to make more robust modeling while indexing the images since it reduces the gap between the low level features and high level content. As a result, more satisfied results to human perception is proposed in retrieval process.

Scene classification is a promising method to model the context in the images since it enables the images to be represented with semantic labels. Therefore, in indexing process of this work, scene classification techniques are used instead of direct local features representation to model the contextual information of the images. Each image is indexed with the probability of observing different semantic classes in it by using the classification results.This indexing structure is used in retrieval process to obtain more satisfactory results.

Scene classification is a difficult problem since determining context of an image depends not only on a single object in it as in object recognition. The context of an image is meaningful when consulting all entities in it. Therefore in order to model the scenes, the descriptors that represent all entities in the images should be used. Early approaches that only look global features extracted on the whole image [13, 30, 9, 7, 31, 34, 33] suffer from the incapability of the global features to derive higher semantic meanings of the images. Recent approaches use local descriptors in scene classification. The common characteristic of these approaches representing the images as histogram of local descriptors. They adapt the traditional “bag of words” document analysis technique to the scene classification as “bag of visterms (visual terms)” [20, 17, 12, 35, 14, 25, 37]. The visual scene descriptors of the images stand for words in the documents here. Each image is modeled as a collection of local descriptors that come from the codebook constructed. Most of the researches use invariant local descriptors called patches to represent the images [20, 17, 12, 14, 25]. However, using patches can give rise to visual polysemy problem since the same patches can be seen in different entities in the images. On this account, more meaningful descriptors for the scenes are used in this work. In order to achieve this, images are segmented into meaningful regions by using color and line structure information of the images. By using the line structures of the images the regions that do not consist of uniform colors such as man made structures are captured. After all regions are clustered, each image is represented with the histogram of the region types it contains. Both multi-class and one-class classification models are used with these histograms to obtain the probability of observing different semantic classes in each image. Since a single class with the highest probability is not sufficient to model image content in an unconstrained data set with a large number of semantically overlapping classes, the obtained probability values are used as a new representation of the images and retrieval is performed on these new representations. For example in Figure 1.1 the graphic shows the probability values of observing different semantic classes in the image.

As seen in the Figure 1.1 the images that are used in the experiments can belong to more than one scene category semantically. While using the probability values in scene classification directly causes classification errors, using them in retrieval process that enables the contribution of each scene category gives more satisfactory results.

Although the probability based modeling reduces the gap between the similarities of the images in feature space and in the human perception, it can not eliminate the subjectivity of human perception. In order to overcome this problem a relevance feedback technique is introduced and the user contribution is included to the retrieval process. According to user feedback the discriminant hyper-sphere is generated to represent relevant images area by using One Class Support Vector Data Description (SVDD) [32]. The images that are relevant to the user are ranked according to the discriminant hyper-sphere and displayed to the user. By this technique, retrieval performance is also increased in addition to its serving to the subjectivity of human perception.

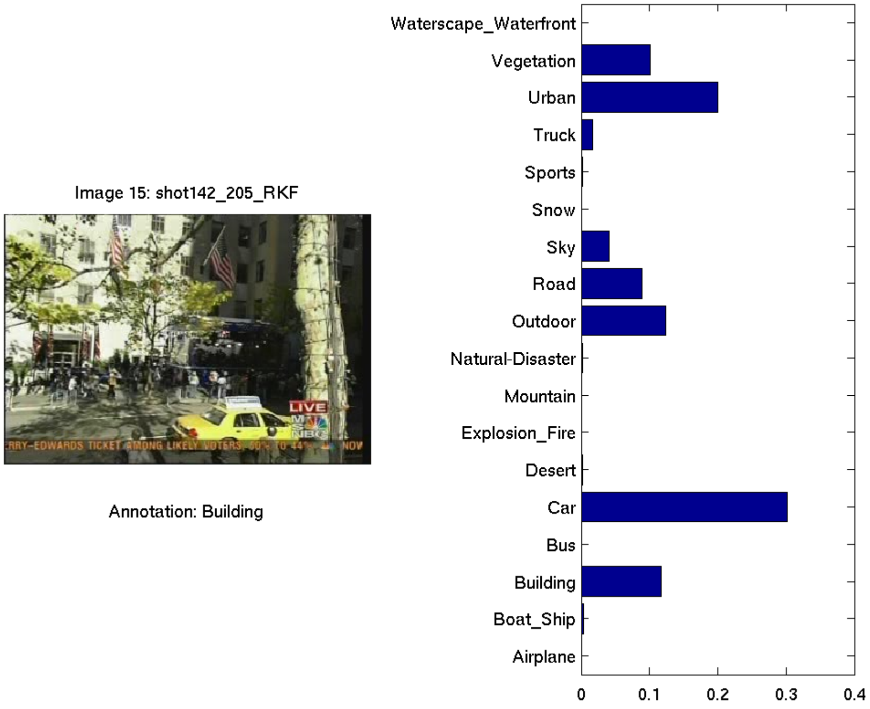

Figure 1.1: Class posterior probabilities of a scene annotated as Building

1.2 Dataset

The performance of the proposed work is illustrated on two different datasets, TRECVID 2005 video shots and COREL dataset. Totally 24517 video shots that are manually labeled into 18 scene categories are used from TRECVID dataset. 16340 of them which are randomly selected from each class are used as training and remaining 8177 shots are used for testing processes. The number of video shots that are used for each class are shown in Table 1.1 with the names of the classes. Figure 1.2 and Figure 1.3 illustrate example shots from each class. Table 1.1 illustrates that the dataset contains semantically overlapping classes. As an example, the outdoor class covers almost all the classes.

Table 1.1: The number of training and testing images that are used for each class from TRECVID dataset

	Training	Testing	Total
Airplane	54	27	81
Boat&Ship	53	27	80
Building	1333	667	2000
Bus	29	15	44
Car	419	210	629
Desert	136	68	204
Explosion&Fire	138	69	207
Mountain	91	46	137
Natural Disaster	47	24	71
Outdoor	6970	3485	10455
Road	550	276	826
Sky	2438	1220	3658
Snow	55	28	83
Sports	398	199	597
Truck	98	49	147
Urban	1527	764	2291
Vegetation	1740	870	2610
Waterscape&Waterfront	264	133	397
Total	16340	8177	24517

Corel dataset contains 4999 images that are composed of 20 natural scene

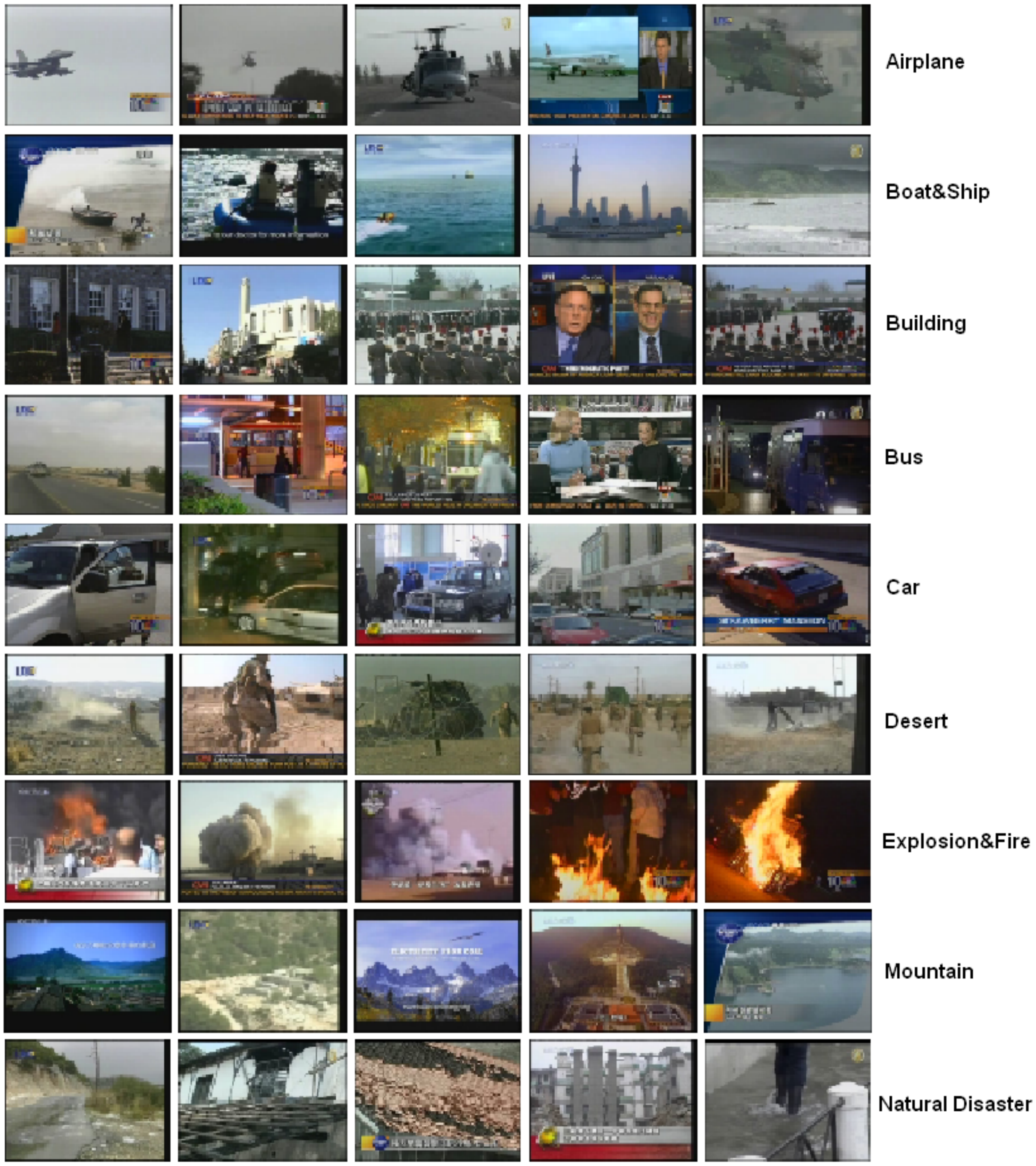

Figure 1.2: Example images from TRECVID dataset for classes Airplane, Boat&Ship, Building, Bus, Car, Desert, Explosion&Fire, Mountain, Natural Disaster.

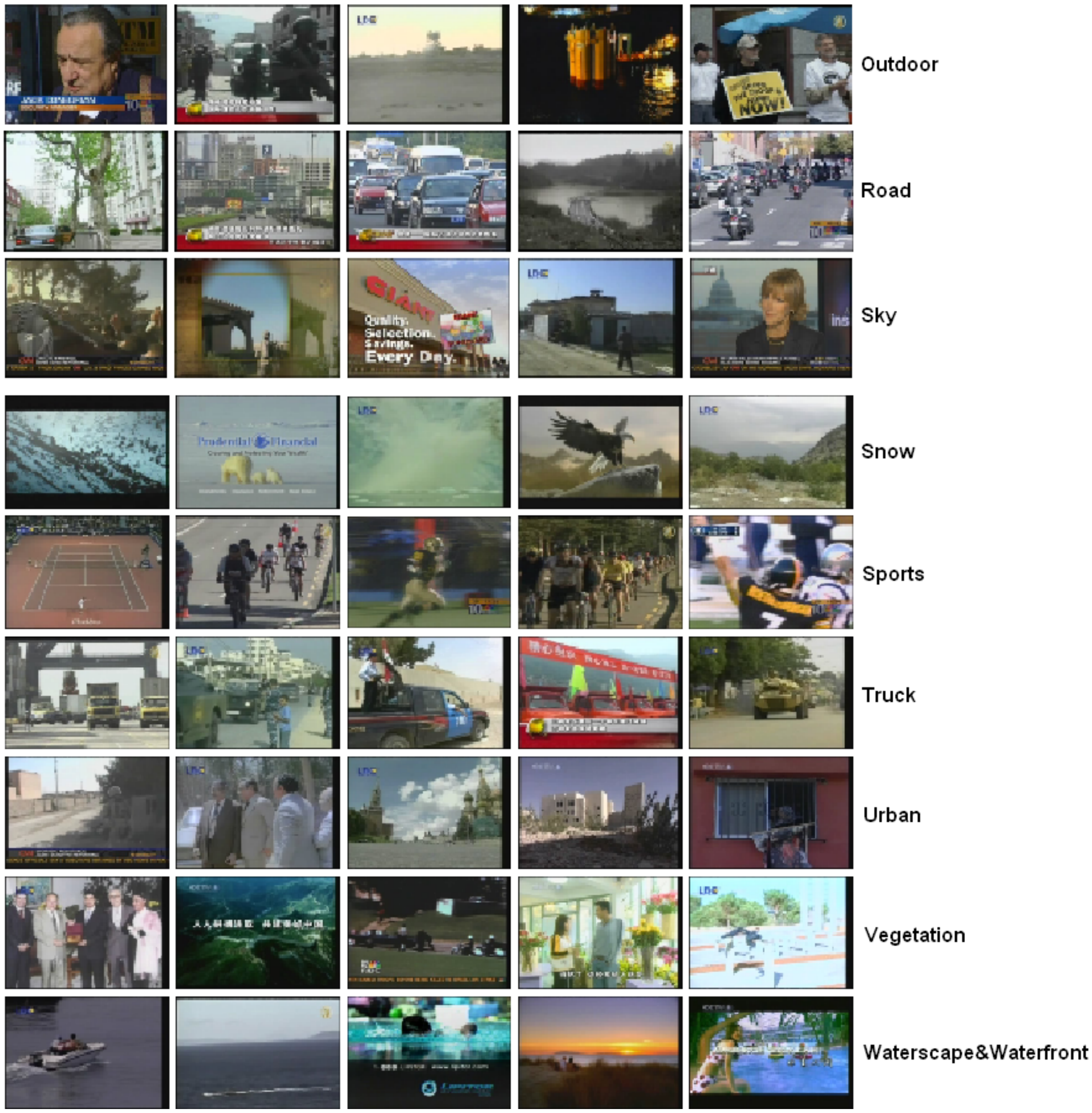

Figure 1.3: Example images from TRECVID dataset for classes Outdoor, Road, Sky, Snow, Sports, Truck, Urban, Vegetation, Waterscape&Waterfront.

categories. Each category of scenes is randomly divided into two sets: 1663 for training and 1663 for testing. The number of images that are used for each scene category is listed in Table 1.2 and example sets for each category are illustrated in Figure 1.4 and Figure 1.5

Table 1.2: The number of training and testing images that are used for each class from COREL dataset

	Training	Testing	Total
Airplane	133	66	199
Boat&Ship	200	100	300
Building	200	100	300
Bus	67	33	100
Car	200	100	300
Castle	200	100	300
Coastal	200	100	300
Desert	134	66	200
Harbor	67	33	100
Mountain	200	100	300
Night	67	33	100
Road	67	33	100
Rock	200	100	300
Ruin	200	100	300
Sky	200	100	300
Snow	200	100	300
Sunset	134	66	200
Surfing	200	100	300
Train	200	100	300
Vegetable	200	100	300
Waterfall	67	33	100

1.3 Summary of Contribution

In CBIR, the image contents are often represented by low-level features that are extracted from the images automatically by using several low-level feature extraction algorithms. However low-level features are no longer sufficient for image

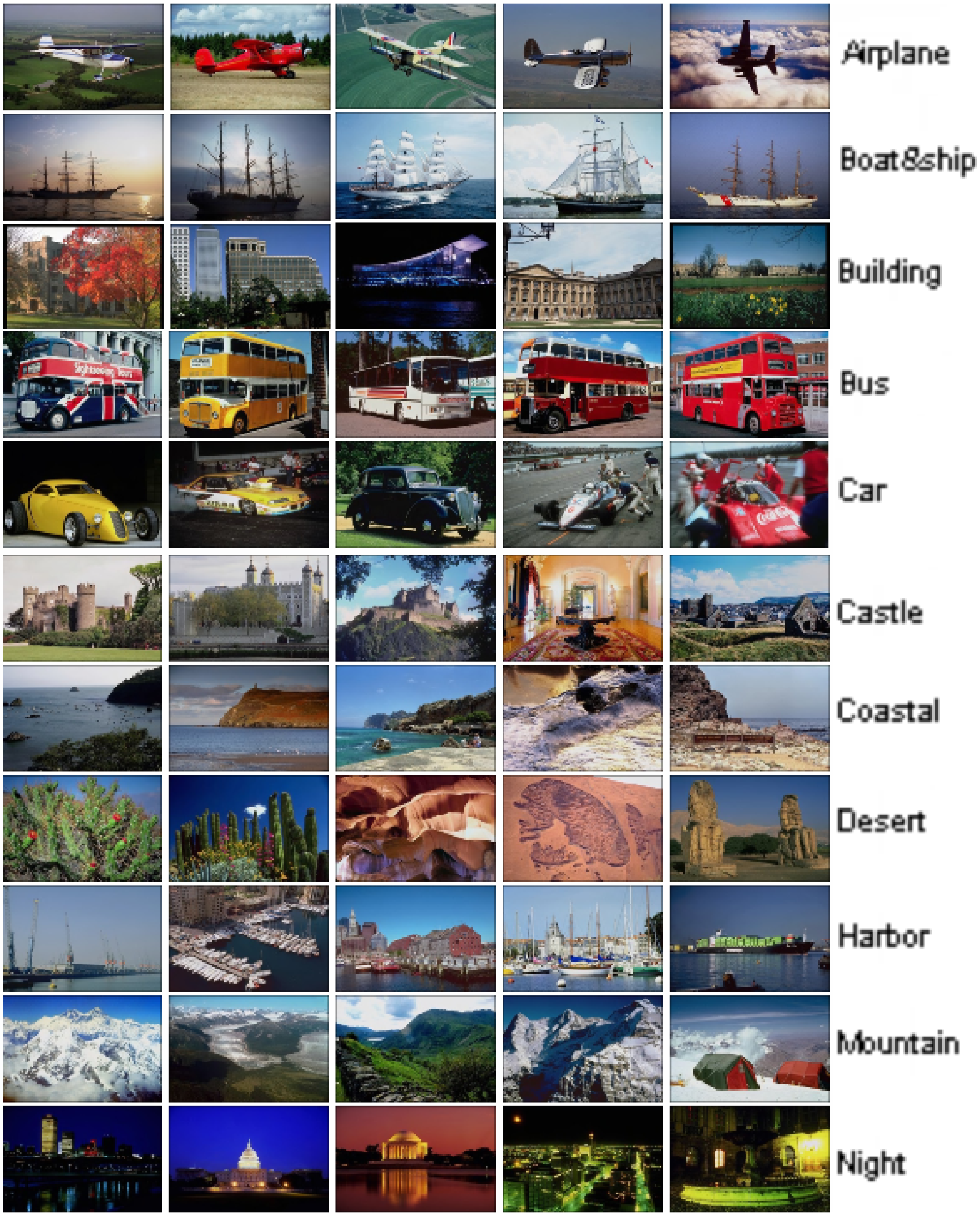

Figure 1.4: Example images from COREL dataset for classes Airplane, Boat&Ship, Building, Bus, Car, Castle, Coastal, Desert, Harbor, Mountain, Night.

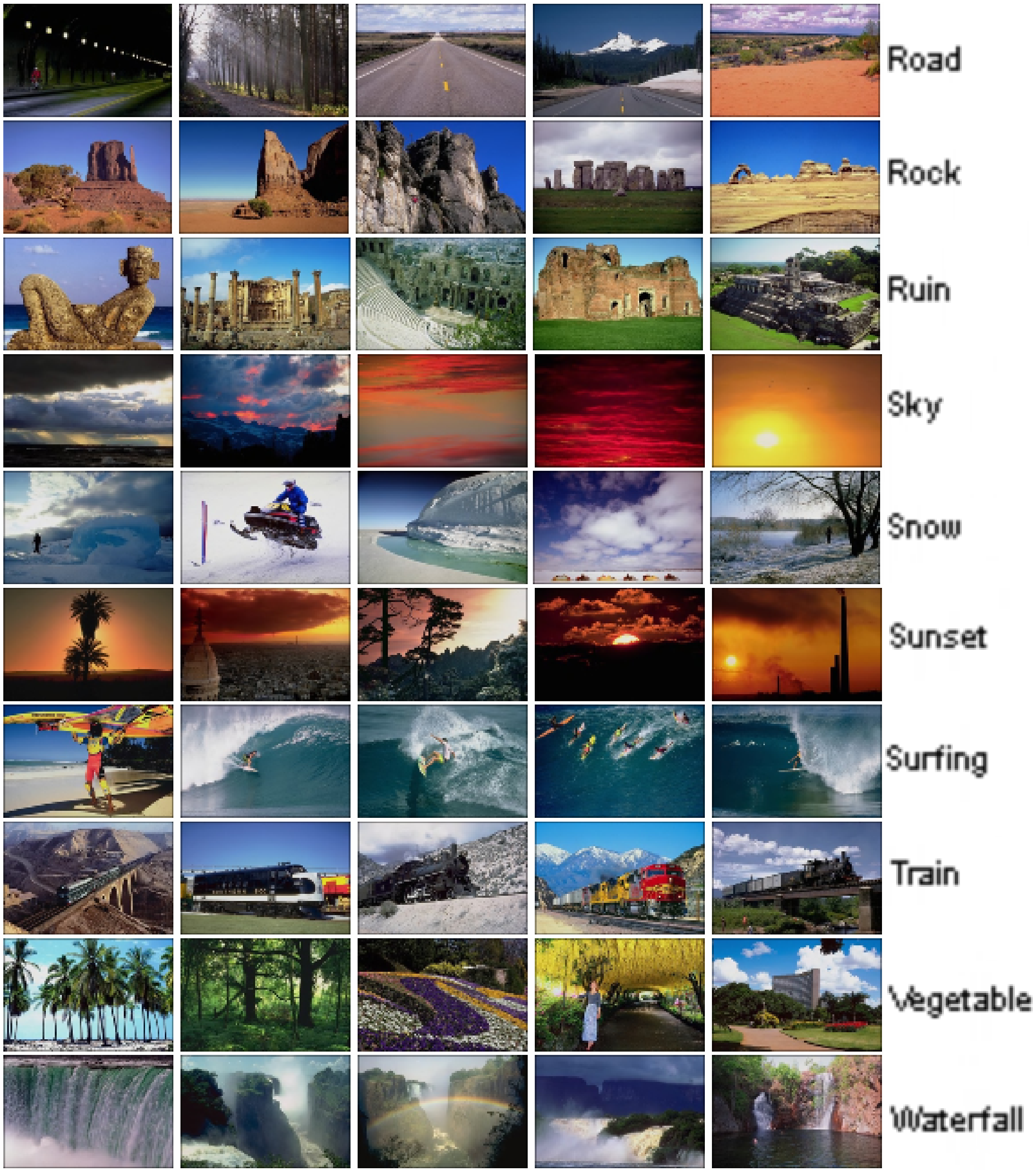

Figure 1.5: Example images from COREL dataset for classes Road, Rock, Ruin, Sky, Snow, Sunset, Surfing, Train, Vegetable, Waterfall.

content representation. In this study each image is represented with the probability of observing different semantic classes in it by using the scene classification techniques and retrieval is performed on these new representations. In order to minimize the semantic gap, a relevance feedback approach that is based on the support vector data description is also incorporated.

1.4 Organization of the Thesis

The organization of the thesis is as follows. Chapter 2 summarizes the related background work about annotation methods and relevance feedback techniques in content based image retrieval. Segmentation of images into regions by using spatial & spectral information and line structure information are described in Chapter 3 and Chapter 4 respectively. In Chapter 5, multi class and one class scene classifications that are used for indexing the images are presented. Chapter 6 introduces a CBIR framework with relevance a feedback technique that is based on one class support vector data description. Chapter 7 contains the experimental results by applying our approaches to TRECVID and Corel datasets. We conclude with a discussion in Chapter 8.

Chapter 2

RELATED WORK

In the literature there are two main approaches in image retrieval according to image indexing method they use. First one is based on representation of the images by a set of keywords that are attached manually to images according to their contents. Queries are created using these keywords. Although efficient image indexing and access tools are available for annotating the images [39], these approaches are not preferable since image annotation is a tedious process. Firstly, it is a hard process to annotate all images of a huge database manually. Second, since a single image may include a multiplicity of contents, and since human perception and understanding vary it is almost impossible for the same images to be annotated with exactly the same keywords by different annotators. The second approach is more efficient than the first one. The images contents are represented by low-level features that are extracted from the images automatically by using several low-level feature extraction algorithms. Most of early approaches have resorted to global feature extraction to represent the images [13, 30, 9, 7, 31, 34, 33]. Vailaya [34] used color histogram, color coherence vector, DCT coefficient, edge direction histogram, and edge direction coherence vector as the features of the image in CBIR. However the global features can not be a solution for the semantic gap between the low level features of the images and high level contents of them. In order to achieve this problem, recent works propose two different types of techniques for CBIR. First one is using local descriptions [10, 27] instead of global ones while indexing the images and the other ones is using learning techniques [40, 8, 21, 4, 6, 23] in CBIR. Whereas Cordelia [27] used local invariant descriptors, Jing [10] used the segmented regions to represent the images. Since the descriptors they use are limited to model the context of the images, to use the performance of contextual information in CBIR many researches apply scene classification techniques to index the images with semantic class information [2, 38, 29, 16, 37]. Carneiro [2] used classification in order to annotate the images and perform retrieval based on this annotation. In order to annotate an image modeled by Gaussian mixture, he used minimum probability error rule based class densities obtained from Gaussian mixture models of images that are annotated with the same semantic class. In the SIMPLIcity system [38] the images are segmented and model-based approach is used to classify the images into basic classes. In CBIR, they used the features that are extracted from the segmented regions based on the classification results they performed. Smith and Li [29] proposed a scene classification method using composite region templates (CRTs) that are generated by using spatial ordering of segmented regions. Then they used classification information in order to index the images. Shapiro [16] used combination of multiple feature types that are extracted from the segmented regions. Multiple types of features are extracted by 3 different segmentation processes based on different context within an image. Then the combination of the features is used for annotation. Vogel [37] used the classification results to rank the images according to their semantic similarities to a semantic class.

When looking more deeply in scene classification recent works use “bag of visterms (visual terms)” technique in classification as mentioned in Chapter 1 [20, 17, 12, 35, 14, 25, 37]. Pedro [25] used difference of Gaussians (DOG) point detector to detect interest points which were used for generating invariant local descriptors. In order to generate patches (invariant local descriptors) Perona [14] used 4 different ways: evenly sampled grid, random sampling, Kadir & Brady saliency detector, Lowe’s DOG detector. For recognition phase they used Bayesian hierarchical models for represent each class. Monay [20] used probabilistic aspect models in addition to “bag of visterms (visual terms)” approach in order to solve the visual polysemy problem. Lazebnik [12] used spatial information of the local descriptors addition to other approaches. She partitioned the images into sub-regions and computed the histogram of the patches inside in each sub-region. Marszalek [17] used spatial information of the patches in order to reduce the influence of the patches that come from the background by giving weights to patches. Gemert [35] and Vogel [37] divided the images in grid cells that are used as visual scene descriptors. Gemert [35] used overlapping grid cells as local descriptors. Gemert [35] thought that choosing a vocabulary to compose codebook is an inherent problem of codebook approach. Therefore in contrast to other approaches they used all vocabulary elements as a codebook.

Relevance feedback is a popular example for the second technique to narrow the gap between the low level features and high level concepts of the images. The typical scenario for relevance feedback in CBIR is as follows:
1. Initial retrieval results are displayed to the user.
2. User gives feedback to the system by selecting the images as relevant or irrelevant according to his/her request.
3. System rearranges the results according to user feedback.

Step 1 and 2 is repeated iteratively until user is satisfied. Several relevance feedback algorithms are proposed in order to perform step 3. The traditional ones are based on assigning weights values to the low-level features and updating them according to the user feedback in CBIR [23, 26, 10]. Another approach called query point movement (QPM) tries to improve the results by moving the query point towards the relevant examples and away from the non-relevant examples [10, 6]. Jing [10] and Giacinto [6] uses Rocchio formula in order to improve the estimate of query point:

$$Q_1 = \alpha.Q_0 + \beta.m_R - \gamma.m_N, \tag{2.1}$$

where Q_1 is the updated and Q_0 is the original query, m_R and m_N means of positive and negative samples provided by user respectively. Rather than a redefining a query, Cox [4] used Bayesian framework to estimate probability distribution over all images and update the distribution according to user feedback. The main problem encountered by these approaches in relevance feedback is small feedback data provided by the user. Guo [8] and Setia [28, 8] tries to solve this problem by using support vector machines (SVM) which generate a discriminant hyper-plane that separates the relevant examples from the non-relevant ones. They updated the hyper-plane according to user feedback. Some researchers try to learn the boundary from only relevant or irrelevant samples and use one class SVM instead of two class [21, 3].

Chapter 3

SEGMENTATION USING COLOR INFORMATION

Scene classification is a difficult problem since determining context of an image depends not only on a single object in it as in object recognition. The context of an image is meaningful when consulting all entities in it. Therefore in order to model the scene of the images the descriptors that represent all entities in the images should be used. Early approaches that only look global features extracted on the whole image [13, 30, 9, 7, 31, 34, 33] suffer from the incapability of the global features to derive higher semantic meanings of the images.

In scene classification phase of this work, “bag of visterm” technique [20, 17, 12, 35, 14, 25, 37], which models the images as a collection of visual scene descriptors, is used. Using invariant local descriptors (patches) [20, 17, 12, 14, 25] as visterms can give rise to visual polysemy problem since the same visterms can be seen in different entities in the images. On this account, more meaningful descriptors for the scenes are used in this work. In order to achieve this, images are segmented into meaningful regions.

Image segmentation is still an unsolved problem in image processing and computer vision. The images that include fewer number of objects in a simple background can be segmented successfully by recent studies. However, estimating common set of parameters makes these studies deficient for large and complex image datasets. Another problem for common segmentation algorithms is using only spectral information of the images. Performing segmentation process only in spectral domain causes noisy structure in the images. Therefore spatial information is also used in addition to spectral information in our approach. In the spectral domain, HSV color values and in the spatial domain position values of the corresponding image pixels are used and these two types of information is combined by combined classifier approach [22].

In the first step of the segmentation, an initial labeling process is performed for the image pixels and a labeled pixel dataset is constructed for each image. After initial labeling step, a new labeling is started iteratively.

The initial labeling is performed by k-means clustering algorithm in spectral (HSV color values) domain and each pixel is assigned to a cluster t, where $t = 1, \ldots, T$. The next labeling step of the initially labeled pixels is performed by using both spectral (HSV color values) and spatial (position values) information. In this step, nearest mean classifier is trained on the spectral domain and Parzen classifier with Gaussian kernel is trained on the spatial domain iteratively. By running the trained classifiers on the same datasets, two class posterior probabilities are computed for each pixel of the image. $P_{spec}(w_t|\mathbf{x}_i)$ and $P_{spat}(w_t|\mathbf{x}'_i), t = 1, \ldots, T$. $\mathbf{x}_i$ is 3 dimensional feature vector that contains HSV values and $\mathbf{x}'_i$ is 2 dimensional feature vector that contains x and y coordinates of the pixel i. For assigning a new label to each pixel both probability values are combined by using the product combination rule:

$$\forall i, i = 1, \ldots, R,$$

$$P_{comb}(w_t|\mathbf{x}_i) = \frac{P_{spec}(w_t|\mathbf{x}_i)P_{spat}(w_t|\mathbf{x}'_i)}{\sum_{k=1}^{T} P_{spec}(w_k|\mathbf{x}_i)P_{spat}(w_k|\mathbf{x}'_i)} \tag{3.1}$$

R is number of pixels in each image. New class label that maximizes the combination probability $P_{comb}(w_t|\mathbf{x}_i)$ is assigned to the pixel i.

This new labeling process is an iterative procedure. At each iteration, the results of spectral and spatial classifiers are combined and new labels are assigned to the pixels by combined classifier until a stable segmentation is reached before

20 iterations. Assume that the label of pixel i at iteration j is λ_{ij}, $j \geq 0$. Then lets define a function $DIFF_{j,j+1}$ that gives number of labels changes between the iterations j and $j+1$.

$$DIFF_{j,j+1} = \sum_{i=1}^{R} I(\lambda_{ij}, \lambda_{ij+1}) \tag{3.2}$$

where I is the indicator function:

$$I(\lambda_a, \lambda_b) = \begin{cases} 1 & \lambda_a \neq \lambda_b \\ 0 & \text{otherwise} \end{cases} \tag{3.3}$$

A stable segmentation is reached if $DIFF_{j,j+1} = 0$ for two consecutive iterations j and $j+1$. The labels of the pixels in the 20^{th} iteration are used if a stable segmentation has not been reached yet.

In most segmentation algorithms the number of regions have to be predefined. However estimating a region number that is suitable for all images in a dataset is considerably hard issue. By using combined classifier approach dynamic region number is attained for each image since after segmentation process there are regions that share same class labels but are located in different locations in the image. Hence, the only parameter that has to be estimated is an approximate value for number of dominant colors, T, which is common for all images.

Since many inhomogeneous color regions are available as well as smooth ones, after segmentation process the segmented images can have many noisy pixels as seen in the second column of the Figure 3.1. In order to eliminate these noisy pixels, a two step filtering process is performed on segmented images. In the first step, the segmented regions that are smaller than a threshold, F, are eliminated and labeled as outlier. In the second step, the regions that are labeled as outlier and smaller than a threshold, B, are merged to their closest neighbor regions. Examples for segmentation and two step filtering processes are shown in Figure 3.1. The original images are given in the first column. The second column shows the segmentation results before applying filtering process. After filtering, the final segmentation results are shown in the last column. The black regions denote the regions that are labeled as outlier. As seen, the regions are captured by this segmentation process are color uniform regions. The entities with miscellaneous colors are eliminated as outlier regions. These types of regions are captured by using their line structural information as explained in the next chapter.

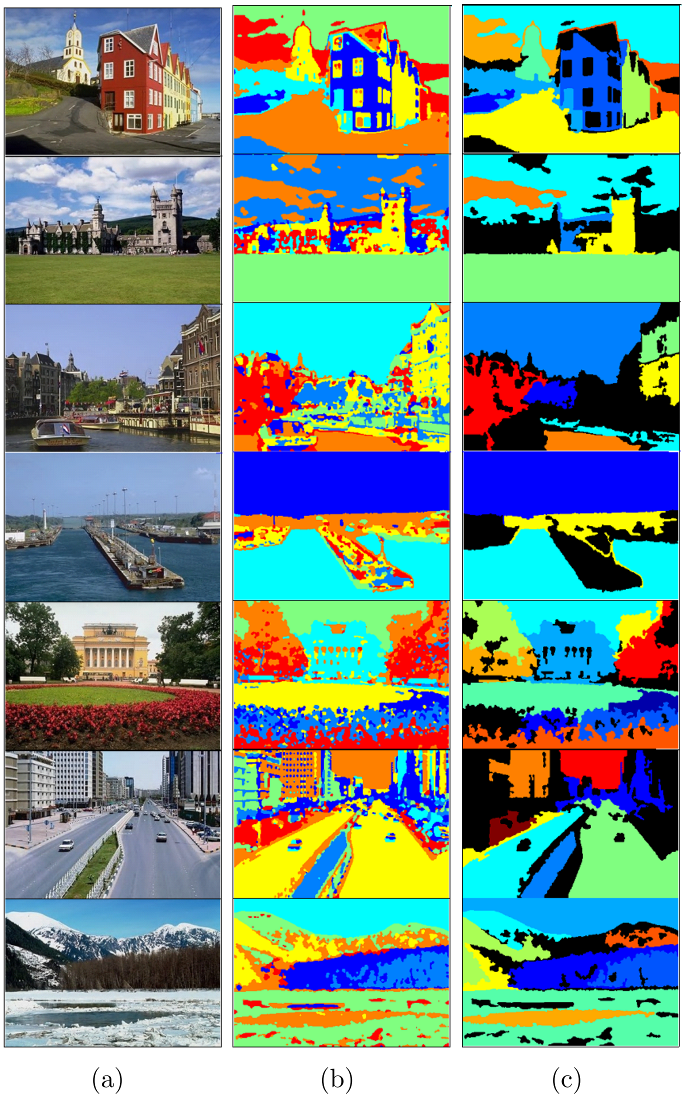

Figure 3.1: Segmentation examples using spatial and spectral information: (a) Original images, (b) Results of segmentation process, (c) Results of filtering process

Chapter 4

SEGMENTATION USING LINE STRUCTURE

Some objects that do not consist of uniform colors can not be segmented by using basically color information of the pixels. The edge structure of the man made objects that includes miscellaneous colors are more distinct feature rather than the color information for them. They generally consist of regular line segments that share common color pairs from two sides (Figure 4.1). In this work, segmentation process is performed by using color information around line segments and the line segments that share common color pairs from two sides are grouped. Since different objects that are close to each other may consist of common colors, their line segments can be located in the same line group.Therefore, presegmented regions are segmented again by using the position information of the line segments. In order to perform segmentation processes hierarchical clustering algorithm is used since constructing hierarchical structure on the line segments allows us to use dynamic number of regions. By deciding the cutting level of the hierarchical structure, suitable number of regions for each image can be estimated.

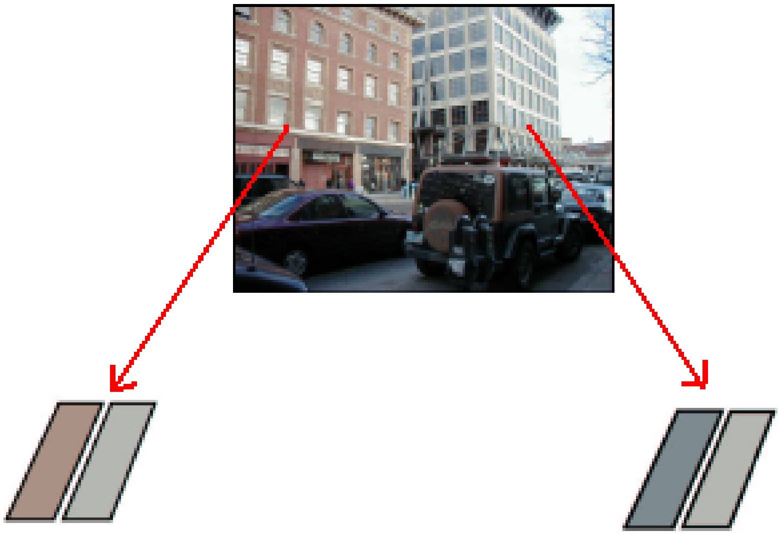

Figure 4.1: Color pairs of two line segment groups (Figure is taken from [15])

4.1 Extracting Line Features

First the edges from the images are extracted by using canny edge detector [1]. Then object recognition tool (ORT) line detector is applied to extracted edges in order to get line segments [5]. The j^{th} line segment, L_{ij} extracted from the image I_i is represented as a feature set with 5 values:

$$L_{ij} = \{\ s_x,\ s_y,\ e_x,\ e_y,\ l\ \}\ i = 1, \ldots, n\ j = 1, \ldots, m \tag{4.1}$$

Above, n stands for the number images in the dataset and m stands for the number of line segments in image I_i. s_x, s_y and e_x, e_y are x and y coordinates of the start and end points of the line segment L_{ij} respectively. Length of L_{ij} is l.

The color information around the line segments that belong to same object are expected to be similar. The line segments of an object usually contain two major colors around them as can be seen in the example in Figure 4.1. Both buildings have two observable colors. One comes from the windows and the other one comes from concrete of the buildings. If we imagine them as line structures we realize that the line segments that belong to same building share two common color pairs one from one side, the other one from other side. Therefore we can say that color information of the line segments is a distinguishing feature for the objects (e.g. man made structures) with regular line segments and miscellaneous colors. This information can be used to segment the images that contain this type of objects into meaningful regions. In order to perform segmentation, first the average RGB color values for defined rectangular regions that cover the line segments are calculated. An example for a rectangular region that covers a line segment with length l is shown in Figure 4.2. It has $2h$ units height.

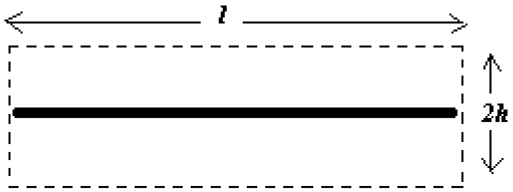

Figure 4.2: Rectangular region around a line segment with length l

Average RGB color values are calculated for two sides of the line segment separately. Therefore, each line segment is represented by 6 color values; 3 of them come from the left and the other 3 come from the right region of the rectangle.

These 6 color values are appended to the previous line feature set Eq. 4.1 and each line segment is represented with new feature set as follows:

$$L_{ij} = \{\ s_x,\ s_y,\ e_x,\ e_y,\ l,\ R_r,\ G_r,\ B_r,\ R_l,\ G_l,\ B_l\ \}\ i = 1, \ldots, n\ j = 1, \ldots, m \tag{4.2}$$

R_r, G_r and B_r are the average RGB values on the right and R_l, G_l and B_l are the average RGB values on the left region of the line L_{ij}.

4.2 Clustering Line Segments

In order to detect the regions that include common line structure, first the line segments in each image are clustered according to their color pairs (Section 4.2.2). In the second phase, position based clustering is performed within the preclustered line segments in order to separate different objects which are close to each other and share common line color pairs (Section 4.2.3). In order to estimate an optimal number of regions for each image, stopping rule technique of hierarchical clustering is used (Section 4.2.1).

4.2.1 Determining Number of Clusters

The main problem in clustering is to decide the number of clusters because the number of objects in an image varies according to the image complexity. Stopping rule for hierarchical clustering is used to estimate an optimum number of clusters for each image [19]. This rule is based on the determination of the cutting level of the dendrogram that is created by agglomerative hierarchical clustering. The dissimilarity matrix of line segments for each image is calculated by using Euclidean distance measurement. Then for each image a dendrogram is created as a result of agglomerative hierarchical clustering. The problem is at which level the dendrogram is cut and which partitions are used as clusters. For example in the Figure 4.3, if the dendrogram is cut at the level between 4 and 5 where the cutting dissimilarity value is 45 then the resulted cluster number is 4. The question is why it is 45. Assume that we have m line segments in image I_i. Then number of levels in the created dendrogram is $m-2$. The stopping rule uses the distribution of the dissimilarity values that are used for creation of the dendrogram at each level. The most appropriate level to cut the dendrogram is the first level j that satisfies:

$$\alpha_{j+1} \;>\; \overline{\alpha} + \; bs_{\alpha}\; j = 1, \ldots, m-2 \tag{4.3}$$

where α_{j+1} represents the distance between the partitions at level $j+1$; $\overline{\alpha}$ is the mean and s_{α} is the unbiased standard deviation of the α distribution; b is the standard deviate which is a threshold that determines how many s_{α} units the α value deviates from the mean, $\overline{\alpha}$. After determining the cutting level j, optimum number of clusters is calculated as $m-j$.

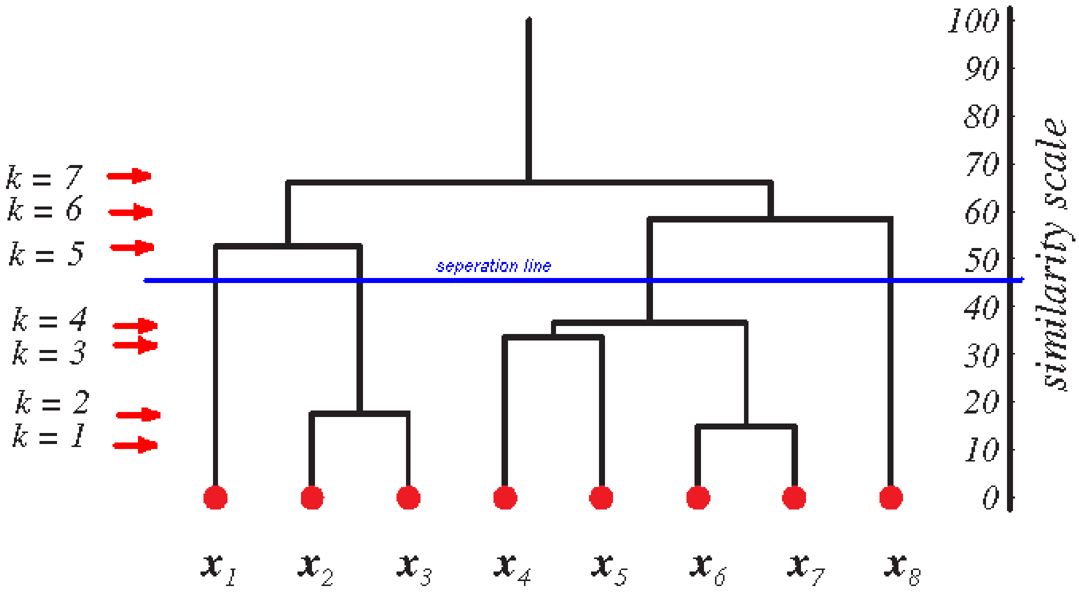

Figure 4.3: Determination of Number of Clusters in a Dendrogram

4.2.2 Clustering According to Color Information

As mentioned the color information around the line segments that belong to same object are expected to be similar. Therefore, the first clustering is performed according to color information of the line segments by using average linkage hierarchical clustering. Using single or complete linkage in clustering can cause some dissimilar clusters to merge due to the outliers they contain. However in average linkage clustering this situation does not occur since each cluster is represented with its average of its members.

By using Euclidean distance measurement, dissimilarity matrix of line segments in each image for hierarchical clustering is calculated. In this calculation 6 color values, $R_r, G_r, B_r, R_l, G_l, B_l$, of the line segments from the feature set Eq. 4.2. Line segments in each image are clustered into an optimum number of clusters that is estimated by the stopping rule of hierarchical clustering as mentioned in Section 4.2.1. The second row of Figure 4.4 shows some examples for clustered lines according to their color pairs (Clusters are shown with unique colored lines).

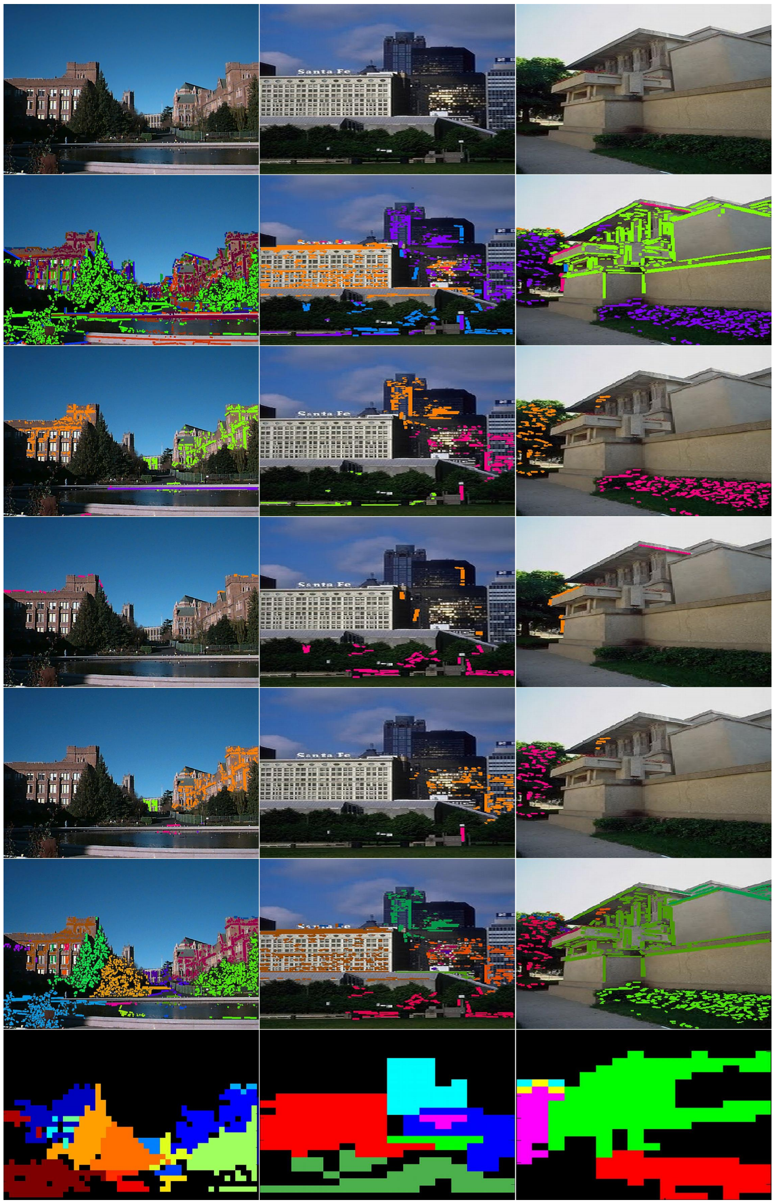

Figure 4.4: Segmentation examples using line structure. First row: original images; second row: result of a color based line clustering; third row: Result of a position based line clustering within one of the color based clusters by average linkage (examples for good clusters); fourth row: Result of a position based line clustering within one of the color based clusters by average linkage (examples for bad clusters); fifth row: Result of a position based line clustering by single linkage; sixth row: Final result of line clustering; seventh row: Regions that are obtained from line clustering (outlier regions are showed with black color).

4.2.3 Clustering According to Position Information

In outdoor images, many different objects have lines with similar color values. As seen in the examples at the second row of Figure 4.4, the lines segments of different entities may still belong to the same clusters. For the first and second example images, the lines of two different buildings belong to the same clusters. In the third example image, it is valid for the lawn part. To rule out such situations, position information of line segments are used. Within the color based line segments they are clustered according to their position information, first using average linkage then single linkage hierarchical clustering algorithms.

4.2.3.1 Step1: Average Linkage Hierarchical Clustering

In order to cluster line segments according to their positions first average linkage hierarchical clustering is used. Average linkage is preferred to reduce the outlier effects of the clusters. To calculate the distance matrix of the line segments both their start and end points are used.

$$D = \begin{pmatrix} d_{11} & d_{12} & \dots & d_{1m} \\ d_{21} & d_{22} & ... & d_{2m} \\ . & . & \dots & . \\ . & . & \dots & . \\ . & . & \dots & . \\ d_{m1} & d_{m2} & \dots & d_{mm} \end{pmatrix}$$

$$d_{ij} = min\{d(\mathbf{s}_i,\ \mathbf{s}_j),\ d(\mathbf{e}_i,\ \mathbf{e}_j)\}\ i,j = 1,..,m \tag{4.4}$$

$\mathbf{s}_i$ is the start point with the coordinates s_{ix} and s_{iy}, $\mathbf{e}_i$ is the end point with the coordinates e_{ix} and e_{iy} of the i^{th} line segment. D is m by m distance matrix of the line segments that are in the same color based cluster. d_{ij} stands for the distance between the i^{th} and j^{th} line segments and take the value of minimum of $d(\mathbf{s}_i, \mathbf{s}_j)$ and $d(\mathbf{e}_i, \mathbf{e}_j)$. $d(\mathbf{s}_i, \mathbf{s}_j)$ and $d(\mathbf{e}_i, \mathbf{e}_j)$ are Euclidean distances of the start and end points of the i^{th} and j^{th} line segments.

After calculating the distance matrix within the color based line segments, clustering is performed by using average linkage hierarchical clustering. Some clusters have a few number of line segments that can not be appropriate to form an object. Therefore some clusters have less than 3 line segments are discarded as a result of elimination process. Third row of the Figure 4.4 shows the results of the position based clustering within one of the color based clusters for each sample image.

Although some resulted clusters have adequate line segments to form an object, their line segments can be too scattered and not exhibit a compact form. These type of line segments usually occur in the boundaries of the objects since the boundary lines share common color pairs one comes from outside, the other from inside of the object. In Figure 4.4, these types of clusters for the sample images can be seen. To rule out this problem a criteria that gives acceptability rate for a cluster is introduced. This criteria is based on the organization of the line segments. If line segments in a cluster exhibit a compact form then this cluster is a good cluster, otherwise, if the line segments exhibit a scattered form then the cluster is a bad cluster. A ratio for each cluster is defined in order to determine this criteria.

$$R_{iv} = \frac{A_{iv}}{M_{iv}} \tag{4.5}$$

where v is cluster id in image I_i; A_{iv} is the area of convex hull that includes all line segments in cluster v; M_{iv} is the number of lines in cluster v. If $R_{iv} > 450$ then the cluster v is not acceptable to represent an object or a region in the image. After applying average linkage hierarchical clustering, the clusters whose R_{iv} ratio is bigger than 450 are eliminated and the next steps are not performed for these clusters. If $R_{iv} <= 100$ then the cluster v is a good cluster. After applying average linkage hierarchical clustering the clusters whose R_{iv} ratio is smaller than or equal to 100 are accepted and the next steps are not performed for these clusters.

4.2.3.2 Step3: Single Linkage Hierarchical Clustering

Sometimes the optimal number of clusters estimated by stopping rule is inadequate to divide line clusters to get the best region representations. Some clusters still have some irrelevant line segments because of color similarity. The form of the clusters are distorted by these irrelevant line segments. This type of clusters are neither in the bad category nor the good one. Their R_{iv} ratio is between 100 and 450 and should be clustered again. Therefore the line segments in these clusters are clustered by single linkage hierarchical clustering. Single linkage similarity method is used this time since the main purpose here is eliminating the outlier lines from the clusters. In the third row of Figure 4.4, the green line segments, which belong to two different buildings exhibit this like of destructed forms. At the fifth row of the Figure 4.4, the results of reclustering step for this cluster can be seen.

The final results of line based segmentation process are shown at the sixth row of the Figure 4.4 for the sample images.

4.3 Representing Line Segment Clusters as Regions

Each line segment cluster represents a region for an image. Segmentation of the images with respect to these line segment clusters is a challenging topic. The first idea that comes to mind is, defining convex hulls which cover all line members of each cluster. However, it causes using of irrelevant area with meaningful regions due to the concave hull structure of the clusters. To rule out this problem a more appropriate method that preserves the form of clusters is introduced. First the images are partitioned into non-overlapping grid cells. Then each grid cell is labeled with the label of the cluster any of whose line member makes an intersection with the corresponding cell. If there is no intersection or the number of intersections in grid cell does not reach a sufficient value then the corresponding cell is labeled as outlier. Finally each line cluster is represented by grid cells as seen at the last row of the Figure 4.4.

Bu using the line structure information of the images, the regions, which are eliminated with color based segmentation process (Chapter 3), are captured. Therefore the meaningful regions, which do not consist of uniform colors and are labeled as outliers are captured in the line structure based segmentation process.

Chapter 5

SCENE CLASSIFICATION

Scene classification is a different research area from the object categorization since in scene classification, determining scene of an image does not depend on fixed content as in object categorization. Contents of an image that belongs to a specific scene can vary. This varied content of the scenes gets scene classification into more challenging problem and the techniques that are used in object categorization can not be used in scene classification. In order to model the scene of an image, visual components that are large enough to represent all entities in the image should be used. Recent approaches use local descriptors as visual components in scene classification. The common characteristic of these approaches is adapting the traditional bag of words document analysis technique to the scene classification as bag of visterms [24, 18, 20, 17, 12, 35, 14, 25]. The visual scene descriptors of the images stand for words in the documents here. Each image is modeled as a collection of local descriptors that come from the codebook constructed. Most of the researches use invariant local descriptors called patches to represent the images [20, 17, 12, 14, 25]. However, using patches can give rise to visual polysemy problem since the same patches can be seen in different entities in the images. On this account, more meaningful descriptors that are obtained as a result of the segmentation process (Chapter 3, Chapter 4) are used in this work.

Another popular problem encountered in scene classification is the restriction of number of classes. Many approaches use limited number of classes in their studies and most of them restrict their studies to two class classification problem. The performed work has dealt with large number of classes. In both datasets, TRECVID and Corel include large number of scene categories. In the following sections the steps in our scene classification algorithm are described.

5.1 Image Representation

The images are represented as a collection of regions that come from the constructed region codebooks.

5.1.1 Region Codebook Construction

In our work two different types of regions are used, one of them comes from color based segmentation and the other one comes from line based segmentation process. Each of these two region collections are represented by different ways and a region codebook is constructed for each of them.

5.1.1.1 Codebook Construction Using Color Based Segmented Regions

The regions which are extracted by color based segmentation process explained in Section 3 are modeled using the multivariate histogram of the HSV values with 8 bins used for the H channel and 3 bins for each of S and V channels, resulting in a 72-dimensional features vector. Then the codebook for k_1 region clusters are learned by performing k-means algorithm on the region features.

5.1.1.2 Codebook Construction Using Line Segment Clusters

Two different representations for line segment clusters are used. One of them is same as the color based region representations. The regions that are obtained by grid cells method explained in Section 4.3 are modeled by HSV histograms as described above (Section 5.1.1.1). The other representation method is based on orientation values of line segment clusters since the color values in a line based region may not be stable. Each line segment cluster is modeled using 10-bin histogram of orientation values of its line segments. These two types of representations are used separately in our work. After the regions are modeled for line clusters, the codebook for k_2 region types is obtained by applying k-means algorithm on the region features.

The codebooks that are generated as a result of two different region types are combined and a new codebook with $k_1 + k_2$ region clusters are constructed.

5.1.2 Image Features

After region codebook is constructed and $k_1 + k_2$ region types are determined, each image is represented as a bag-of-regions as below by calculating histogram of the region types it contains.

$$I_i = \{r_{i1}, \ldots, r_{it}\} \tag{5.1}$$

where $\{r_{i1}, \ldots, r_{it}\}$ are the regions the image I_i contains and t denotes the number of regions in image I_i.

5.2 Classification

For probability estimation two different classification models are used: multi class and one class. In both settings, the goal is to estimate the posterior probabilities $P(w_j|r_1, \ldots, r_t), j = 1, \ldots, c$, where w_j represents the jth class, c is the number of classes.

5.2.1 Multi Class Scene Classification

The images are classified using the Bayesian decision rule according to posterior probabilities. The image with the set of regions $\{r_1, \ldots, r_t\}$ is assigned to the class

$$w_j^* = \arg \max_{j=1,\ldots,c} p(w_j | r_1, \ldots, r_t) \tag{5.2}$$

where w_j represents the j^{th} class, c is the number of classes, and t is the number of regions in the scene. Using the Bayes rule, the posterior probabilities can be computed as

$$P(w_j | r_1, \ldots, r_t) = \frac{P(r_1, \ldots, r_t | w_j) P(w_j)}{P(r_1, \ldots, r_t)}. \tag{5.3}$$

Assuming equal priors for all classes, the classification problem reduces to the computation of class-conditional probabilities $P(r_1, \ldots, r_t | w_j)$.

Each region is assumed to be independent of others given the class. Therefore class conditional probability can be calculated as

$$P(r_1, \ldots, r_t | w_j) = \prod_{i=1}^{t} P(r_i | w_j). \tag{5.4}$$

The probability of region r_i having label u is computed as

$$P(r_i = u | w_j) = P_{ju} = \frac{n_{ju}}{n_j}. \tag{5.5}$$

where $u \in 1, \ldots, k_1 + k_2$, $j = 1, \ldots, c$, n_{ju} is the number of regions with the label u in the training set for class j, and n_j is the total number of regions in the training set for class j.

5.2.2 One Class Scene Classification

Since the scene classes may not be mutually exclusive, the multi class classification is not always suitable. Therefore one class classification has also been used and each class is independently modeled. Assuming all classes in the training set form a normal distribution, classifiers that estimate a Gaussian density on each class are trained. Therefore probability density function for the j^{th} class can be calculated from the following equation:

$$P(x|w_j) = \frac{1}{(2\pi)^{\frac{d}{2}}(\Sigma_j)^{\frac{1}{2}}} e^{\frac{-1}{2}(x-\mu_j)^T(\Sigma_j)^{-1}(x-\mu_j)} \tag{5.6}$$

where x is the histogram vector of region types with length $k_1 + k_2$ for an image in j^{th} class, μ_j and Σ_j are the mean and covariance matrix of the j^{th} class. These are estimated from the training samples. The test images can be classified according to posterior probabilities

$$P(w_j|x), \qquad j = 1, \ldots, c \tag{5.7}$$

and again from the Bayes rule, assuming equal priors for all classes, the classification problem reduces to $P(x|w_j)$.

The images that are used in the experiments can belong to more than one scene category semantically. For instance, the example images in Figure 5.1 can not belong to exactly one scene category. The graphical representations of the class probability values of each image are shown on the top.

As seen in the Figure 5.1 the probability values for the scenes that images can belong to are similar to each other. Whereas assigning the first two images to the scene categories with the maximum probability gives successful results, for the last two images, using probability values results in failure in classification. For example the third image which is annotated as Boat&Ship, will be labeled as WaterScape&Waterfront in classification process, although the probability of belonging to Boat&Ship class is high.

Therefore instead of assigning strict labels to the images, they have been modeled with their class posterior probabilities and the models are used as indices of the images in retrieval process. Thanks to this method, contribution of each scene category can be used for representing the images.

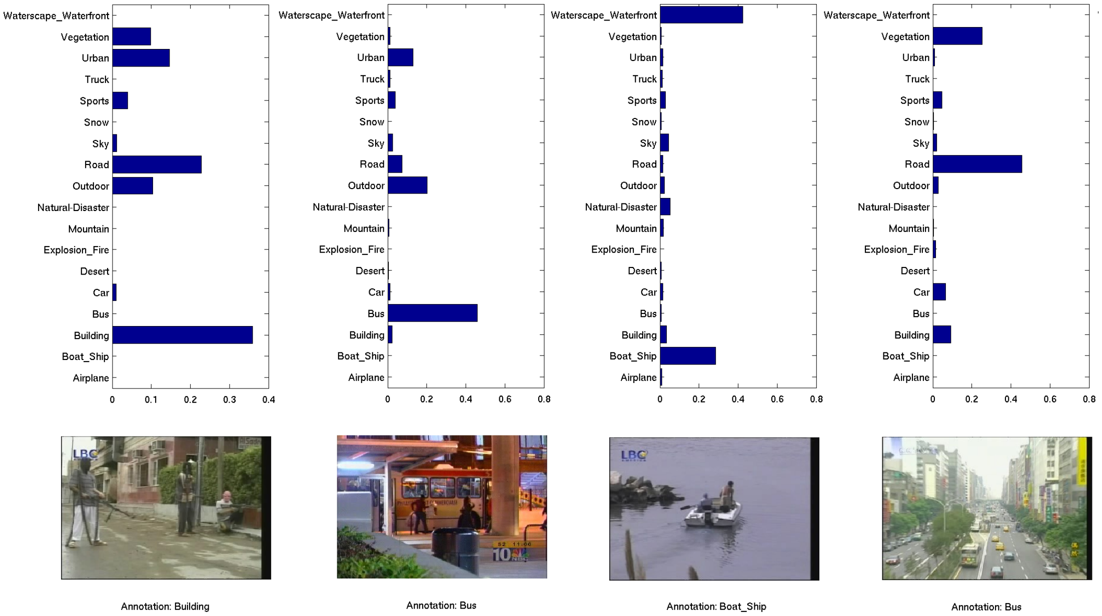

Annotation: Building

Annotation: Bus

Annotation: Boat_Ship

Annotation: Bus

Figure 5.1: Class posterior probabilities of scenes for example images

Chapter 6

CONTENT BASED IMAGE RETRIEVAL WITH RELEVANCE FEEDBACK

In content based image retrieval there is always a gap between the high level semantics of the images that human perceives and the low level features of the images that machines compute. In order to deal with the semantic gap problem various relevance feedback algorithms are proposed in the area of content based image retrieval and include the user in retrieval process. In most common techniques, user judges the retrieved results as relevant or non-relevant to the query image. Then new results are calculated by using the feedback of the user. The user applies feedback until getting satisfactory results. There are various algorithms for recalculation of new results according to user feedback. The main problem encountered in relevance feedback approaches is small feedback data provided by the user. Some approaches tries to solve problem by using classification techniques. One of the most popular techniques is using support vector machines (SVM) which generate a discriminant hyper-plane that separate the relevant examples from the non-relevant ones [28, 8]. Then the images that are in the relevant side are reranked according to distance to the hyper-plane in descending order. The major stumble in this approach is treating the problem as two class classification problem. It is straightforward to assume that all relevant images belong to the same class. On the other hand, the classes of non-relevant images probably vary. Hence forcing to assign them to the same class decreases the retrieval performance. In this work, to deal with this problem a relevance feedback approach is proposed by using one class data description technique, Support Vector Data Description (SVDD) [32, 21]. One class SVDD is inspired by Support Vector Classifier and can be used for classification where one of the classes is sampled well and the other one is not. SVDD generates a discriminant hyper-sphere that can separate the target class from the outliers. Detailed description about SVDD is explained in Appendix A.

In our work, the relevant images that user presents are used as target samples and non-relevant images as outliers. While SVDD tries to find a hyper-sphere which contains most of the target samples, by using non-relevant samples it tries to minimize the volume of the sphere in order not to include any superfluous space. Therefore, it uses also outliers to find a more efficient description [32].

In retrieval scenario, using region histogram features as image features is not an effective way to represent the images since the number of region types that an image includes is very small related to the total number of region types. Therefore, the images are modeled with class posterior probability values that come from classification process for each class.

In the first retrieval process, the images are sorted according to the posterior probability values of the scene class that user searches for and displayed to the user. After obtaining a feedback from the user an optimum hyper-sphere is generated by SVDD that separates the relevant samples from the non-relevant ones. Then again the images in the relevant area are ranked in decreasing order according to the distance to the hyper-sphere. After the images in non-relevant area are ranked in increasing order according to the distance to the hyper-sphere, they are appended to the first ranking group (Figure 6.1). Then the results are shown to the user to obtain a new feedback until a satisfactory result is reached. Whole retrieval scenario with relevance feedback is shown in Figure 6.2.

Relevance feedback technique also solves the problem that grows out of class

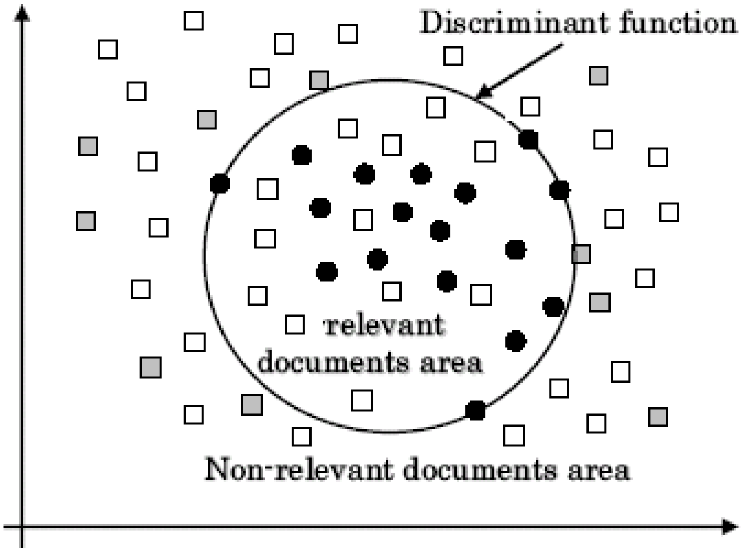

Figure 6.1: Generation of a hyper-sphere to discriminate relevant images area by SVDD: Black circles denote relevant and gray boxes denotes the non-relevant images are evaluated by the user. Empty boxes are the displayed images that are not checked. (Figure is taken from [21])

overlapping since by giving the individual contribution, the user eliminates the visual polysemy in his/her point of view.

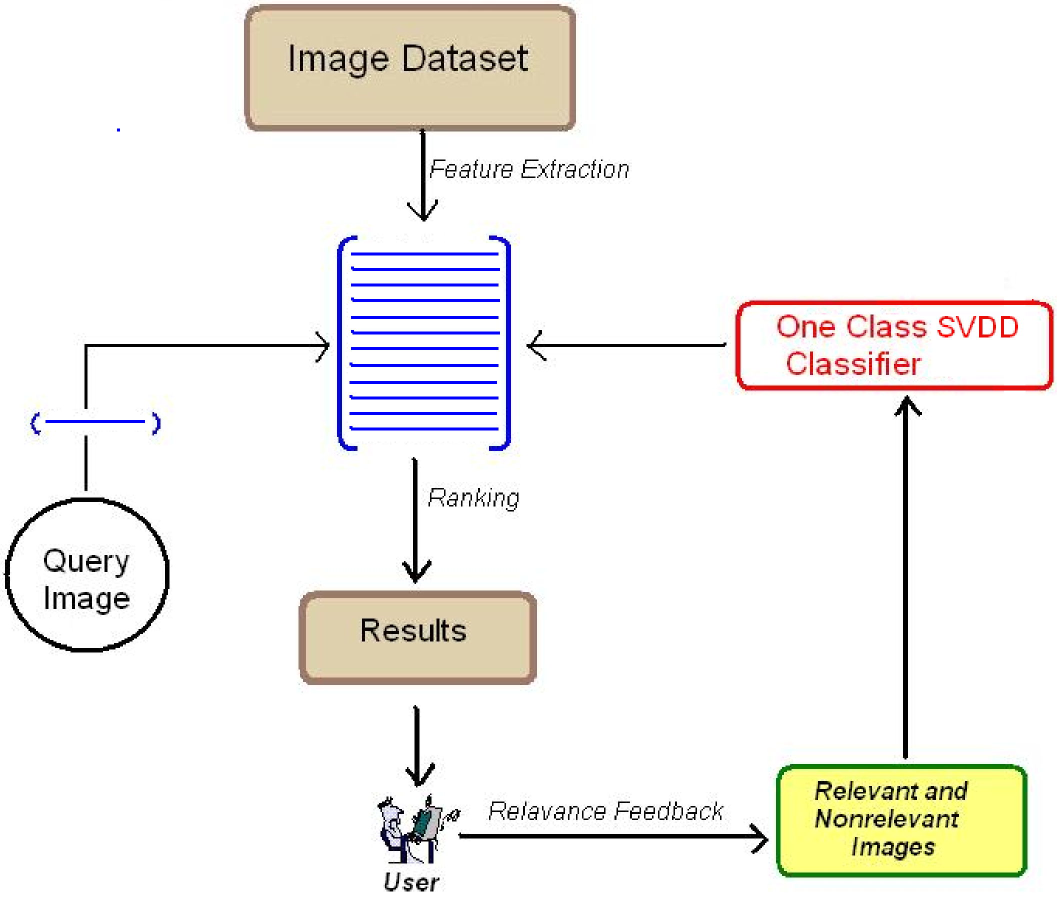

Figure 6.2: Relevance Feedback Scenario

Chapter 7

EXPERIMENTS

7.1 TRECVID

7.1.1 Classification

A codebook has been learned from the regions that are extracted from whole dataset by a segmentation process. Because of crowded and complex structure of the images in TRECVID dataset, line based segmentation process gives bad performance on this dataset. Therefore, the segmentation has been performed by using only color information (Chapter 3). The values of 5, 7 and 10 are used for T. The value 7 has been selected for T as a result of observations on a randomly selected sample dataset. The elimination process, which is the last part of segmentation, is performed by using values 2000 for F and 100 for B. The codebook is constructed from the regions that are modeled by HSV color histograms by using the values 100, 500 and 1000 for k_1. Two type of models for each category of scenes have been obtained from the training images. One of the models is created by using multi class classifier and the other is created by using one class classifier that fits Gaussian model on each class independently. One class classifier has been used in order to eliminate classification errors arise from class overlapping problem. The value 1000 for k_1 gave the best classification results for both model types as seen in Table 7.1.

Table 7.1: Classification success rates for different k_1 values for both multi class classifier and one class classifier models

	Multi Class	One Class
$\mathrm{k}_1 = 50$	%18	%13
$\mathrm{k}_1 = 200$	%25	%12
$\mathrm{k}_1 = 500$	%32	%10
$\mathrm{k}_1 = 1000$	%38	%10

Confusion matrices for classification result are illustrated in Figure 7.1 for both types of models. On the confusion matrices each column represents the instances in the predicted class and each row represents the instances in an actual class. Overall classification accuracies are 16.57% and 10.26% for Figure 7.1(a) and Figure 7.1(b), respectively.

The low performance for multi class classification is obtained for “outdoor” and “sky” classes as seen in the confusion matrix in Figure 7.1. These are the expected results for the scene categories that enclose other scenes semantically. Most of the images in TRECVID dataset are outdoor images and include sky scene. There is also class overlapping problem for all other scene categories. Necessity of assigning each image, which can belong to multiple scene categories but annotated with one of them, to a single class reduces the success rates dramatically. The last two images in the Figure 5.1 of Chapter 5 is an evidence of this situation. The third image, which is annotated as Boat&Ship, is predicted as WaterScape&Waterfront in classification process since it should be assigned to the class with the maximum probability. Since “outdoor” is more general scene category, in one class model there is also instability problem for the number of class instances. Number of instances in the “outdoor” class exceeds all other class populations. Therefore, the Gaussian model for the “outdoor” class encapsulates most of the images in other classes. Although it is an expected situation, it raises problems in classification process. As seen in confusion matrix in Figure 7.1(b) most of the images in different categories are predicted as “outdoor”

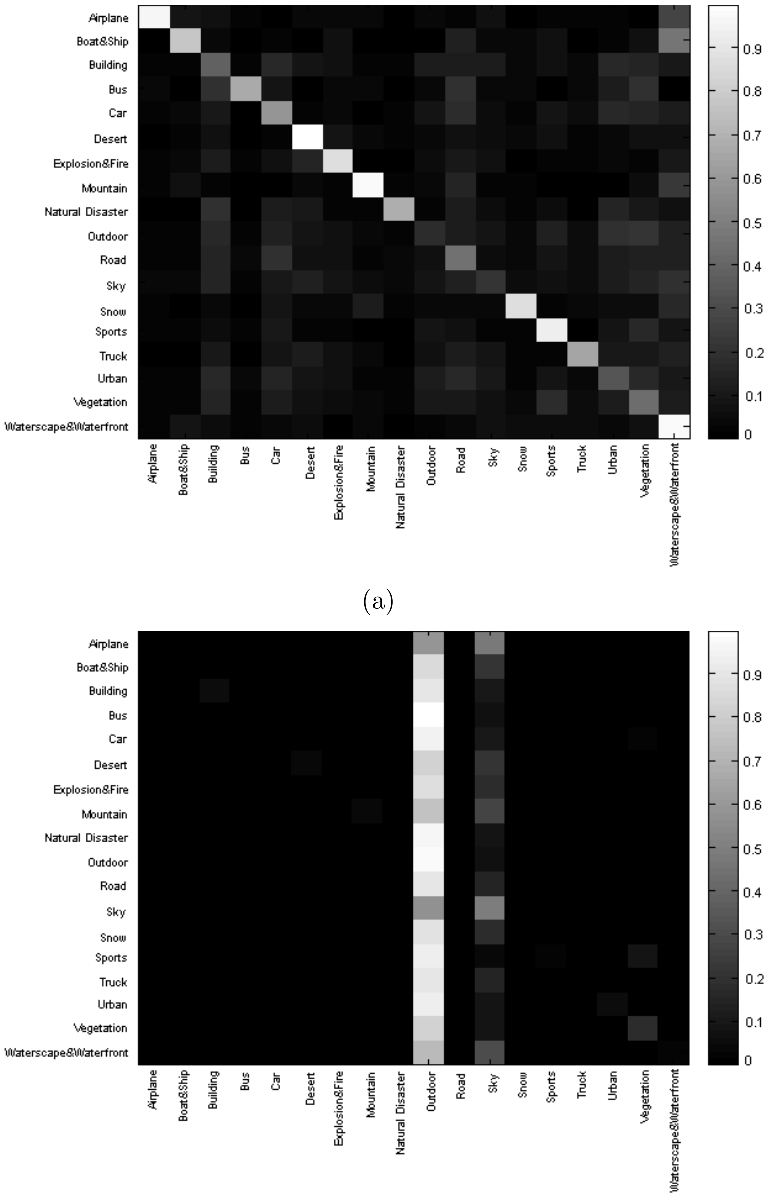

(a)

(b)

Figure 7.1: Confusion matrices of TRECVID for two different models: (a) Confusion matrix for multi class classifier model, (b) Confusion matrix for one class model

since TRECVID dataset consists of outdoor images. In confusion matrix, the other scene category dominates others is “sky”. It is an expected situation since most of outdoor images include sky but the results are reflected as classification errors.

In order to show the performance of probability model we sort the images according to class probabilities for each category then we calculate mean average precision (MAP) values using this ranking (Figure 7.2). For multi class classification model (Figure 7.2(a)), MAP values are above 0.5 for all classes. As seen in Figure 7.2(a) and Figure 7.2(b), the performances of both multi class and one class models are very high for “outdoor” and “sky” classes.

7.1.2 Retrieval with Relevance Feedback

Instead of using class probabilities obtained from classification process, they are used for image representation in a retrieval process. Each image is represented by a vector whose components are class posterior probabilities for each scene category. The classification results are used for generating queries automatically and ground truth is used for providing feedback to the system. Quarter of the images of each class population is used as query images. For each query, the top 30 images are employed for providing feedback by automatically labeling each image that belonged to the same ground truth group with the query as relevant and the remaining images as irrelevant at each iteration. This process is repeated for each selected query image for 4 feedback iterations. Figure 7.3 shows precision plots of the original retrieval and the following 4 iterations for multi class and one class classifier models. Figure 7.4 illustrates the mean average precision values (MAP) of each scene category again for multi class and one class classifier models. MAP values are calculated for the original retrieval and the following 4 iterations. For both of the models the first iteration gave the largest increase in precision. A little rise is obtained for the next 4 iterations. The precision values for one class classification model is much higher than the multi class classification model since while calculating the posterior class probabilities for overlapping classes, learning a boundary for each class that separates it from

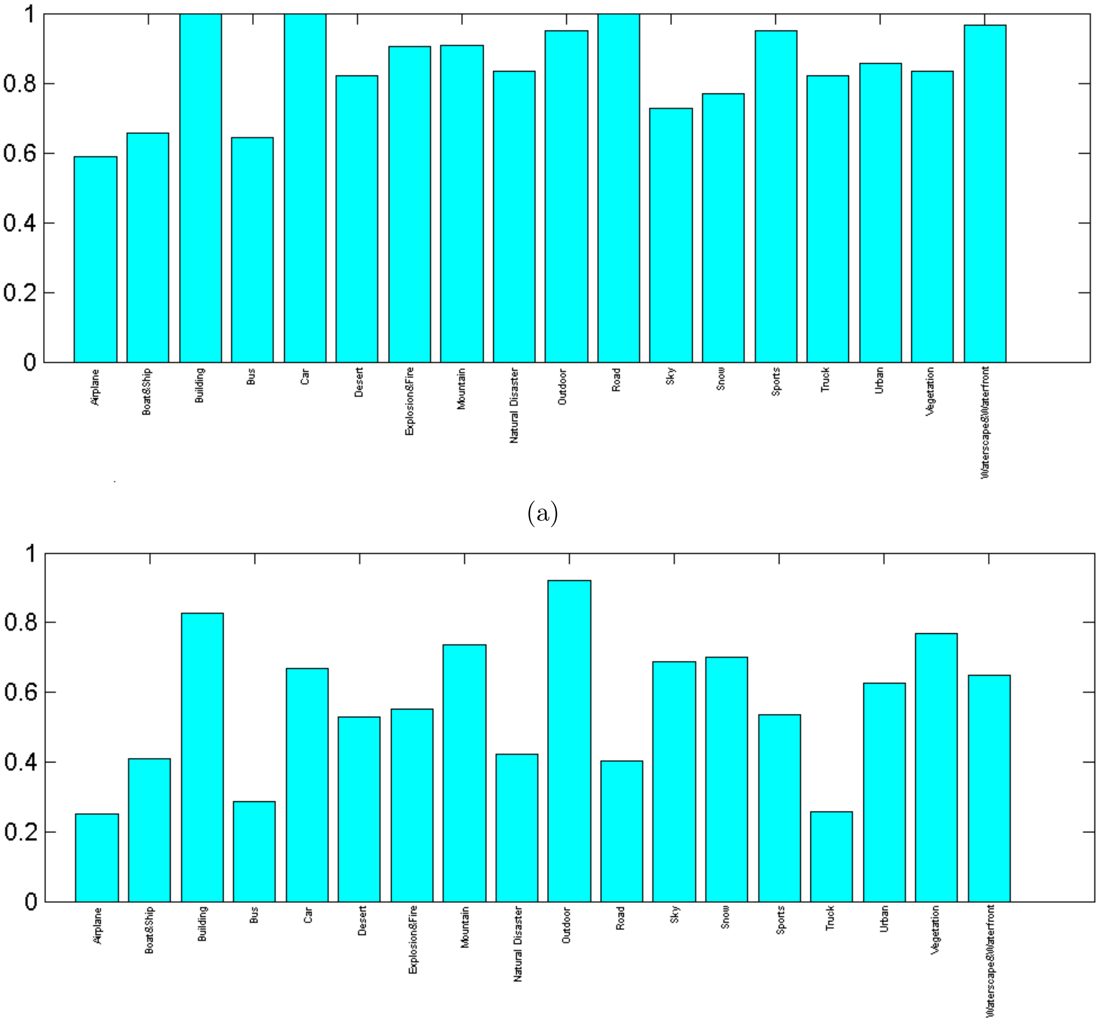

(a)

(b)

Figure 7.2: Mean average precision values (MAP) according to class posterior probabilities of each scene category of TRECVID dataset: (a) MAP values for multi class classifier model, (b) MAP values for one class classifier model.

the others is more efficient than learning a boundary that separates all the classes from each other. In TRECVID dataset the big problem is existence of "outdoor" class. It is almost impossible to represent the "outdoor" scene category with multinomial model since it can not be separated from the other classes. Both results are more acceptable than the classification results since the contribution of each of 18 scene categories are used in image representations. Since high precision values have been already reached in the first retrieval, satisfactory increases can not be obtained for feedback iterations. TRECVID dataset is a hard dataset for classification. Images in TRECVID dataset have complex background with multiple contents and it is not possible to assign them to a single class. In order to retrieve more realistic performance, we annotate the images with multiple class labels to use in retrieval process. While calculating the precision values, we use all possible class labels of the images. This is the main reason that the retrieval performance is higher than the performance of COREL dataset which will be explained in the next Section 7.2.

7.2 COREL

7.2.1 Classification

For COREL dataset the codebook is generated by using the regions that are obtained by both color based and line based segmentation processes. The value of $1.6l$ is used for h, to create the rectangle that surrounds a line segment which has a length l. In order to determine the the number of line clusters, stopping rule is applied to the line clustering using the value 4 for b. The color based segmentation and elimination processes are performed with the same parameters as the parameters that are used in TRECVID dataset. Two types of codebooks are constructed from the color based and line based regions. The regions from the codebook, which is obtained by the color based segmentation, are modeled by HSV color histograms. Region clustering uses 1000 for k_1. The regions from the codebook, which is obtained by line based segmentation, are modeled by both

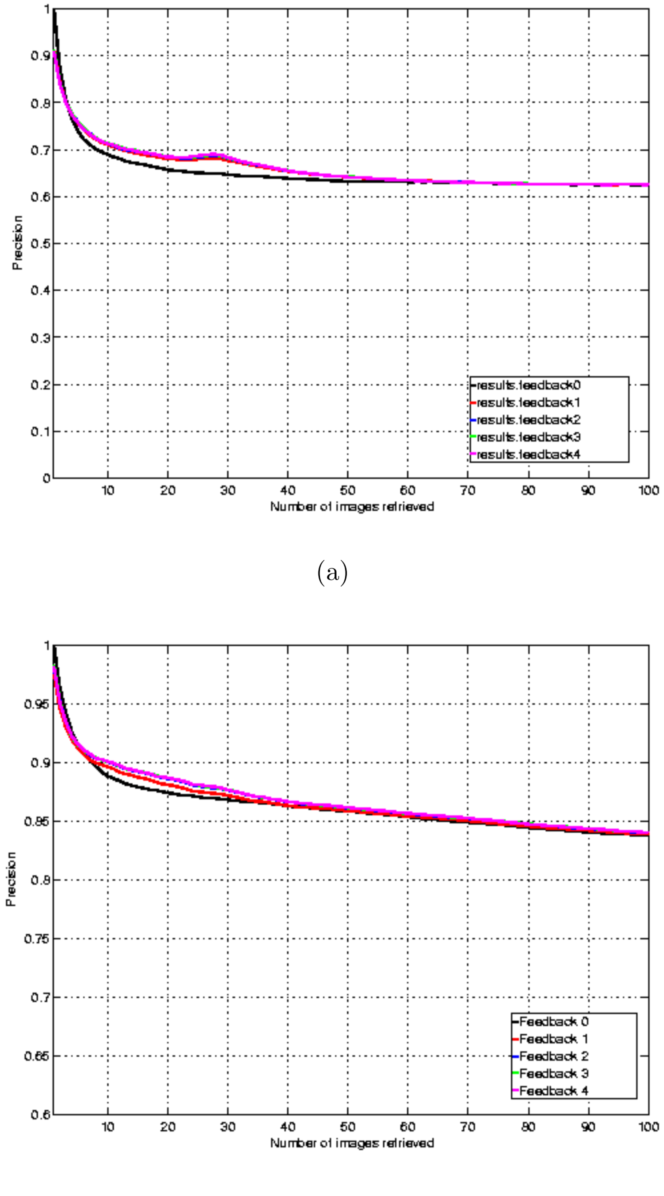

(a)

(b)

Figure 7.3: Precision vs. number of images retrieved plots of TRECVID for two different models. ‘Feedback 0’ refers to the retrieval without feedback: (a) Precision plot for multi class classifier model, (b) Precision plot for one class classifier model

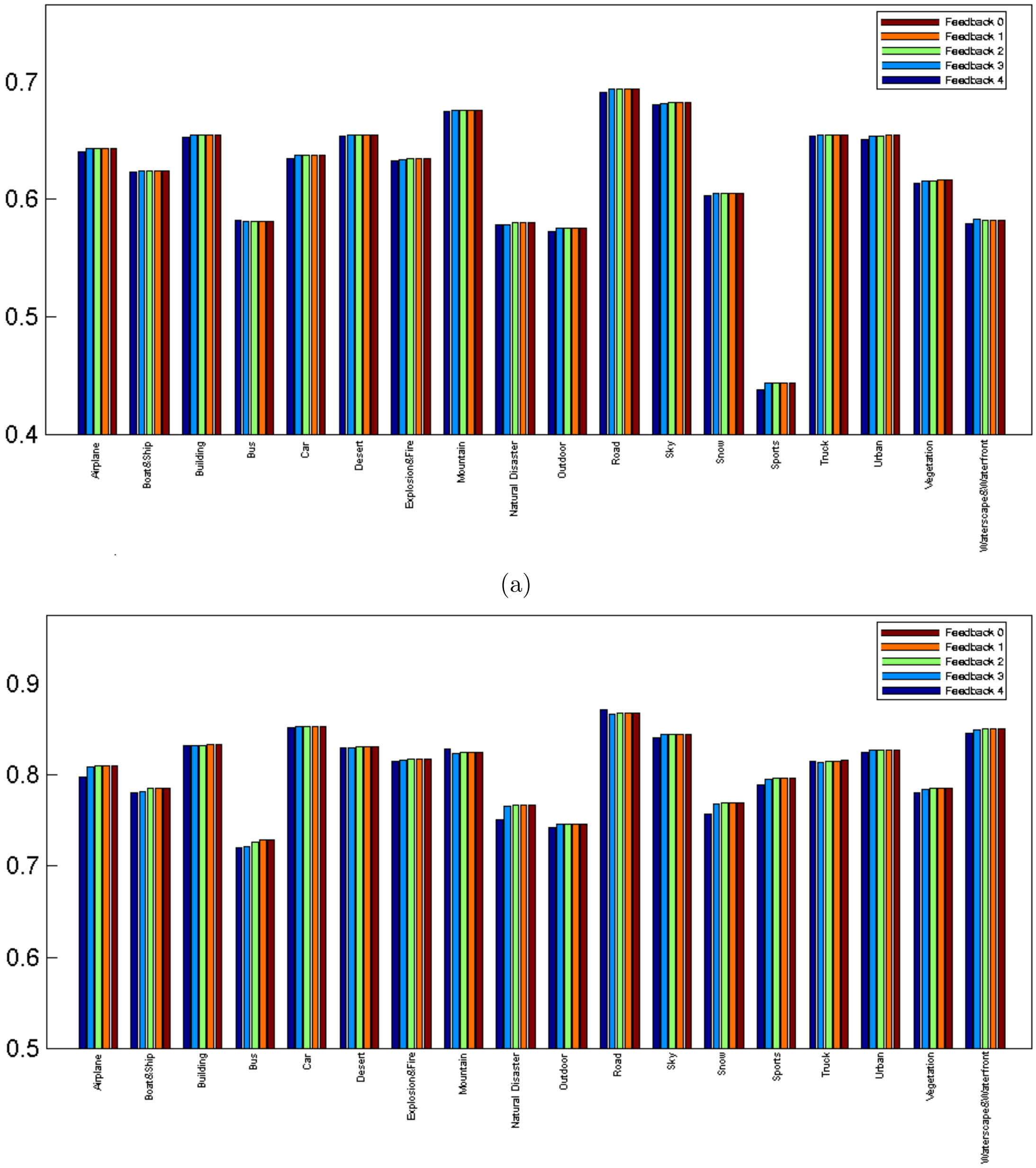

(a)

(b)

Figure 7.4: Mean average precision (MAP) graph of each scene category of TRECVID dataset for the original retrieval and the following 4 iterations. 'Feedback 0' refers to the retrieval without feedback: (a) MAP graph for multi class classifier model, (b) MAP graph for one class classifier model

HSV color histograms and orientation histograms of the line segments in the regions. As a result, two types of codebooks with size $k1 + k2 = 2000$ are obtained, one is a combination of color based regions that are modeled by HSV histograms and line based regions that are modeled again by HSV histograms, the other one is a combination of color based regions that are modeled by HSV histograms and line based regions that are modeled by orientation histograms of the line segments. For classification process only multi class classifier is used for modeling the scene categories since in COREL dataset there is not a scene category as "outdoor" that encapsulates the other classes. Therefore we do not get better results from the experiments that are performed using one class classifier. Figure 7.5 shows the confusion matrices for classification results of each type of codebook representations. Overall classification accuracies are 61.35% and 34.76% for Figure 7.5(a) and Figure 7.5(b), respectively.Since there are large number of scene categories and these categories are not mutually exclusive semantically, we do not expect satisfactory results in classification. For example a mountain scene, a sky scene and a waterfall scene can take place at the same image. Instead of assigning the images that are modeled by posterior class probabilities to a single class, we attempt to use these probability values to show the performance of the model. We sort the images according to their class probabilities for each category then we calculate MAP values using this ranking (Figure 7.6). The MAP values are very high for all classes for both codebook types. These values verify the suitability of our representation technique in modeling the visual content of the images. It is adequate to represent the images with the contribution of each scene category to perform retrieval process.

7.2.2 Retrieval with Relevance Feedback

The same processes as TRECVID dataset for content based image retrieval are applied to COREL dataset by using class posterior probability representations of the images. Figure 7.7 shows precision plots of the original retrieval and the following 4 iterations for the codebook based on HSV histograms and the codebook based on the combination of HSV and orientation histograms. Figure 7.8

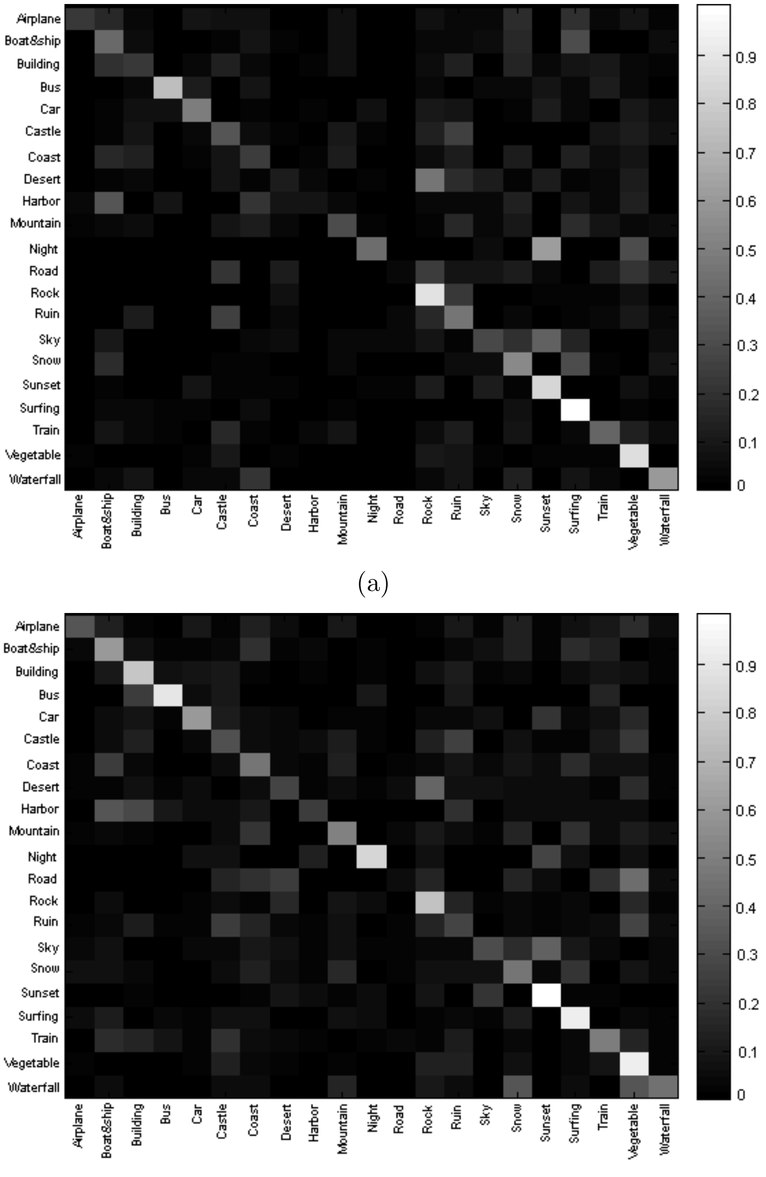

(a)

(b)

Figure 7.5: Confusion matrices of COREL for two different codebook types: (a) Confusion matrix for the codebook that is constructed by using HSV histograms of the regions, (b) Confusion matrix for the codebook that is constructed by using HSV and orientation histograms of the regions

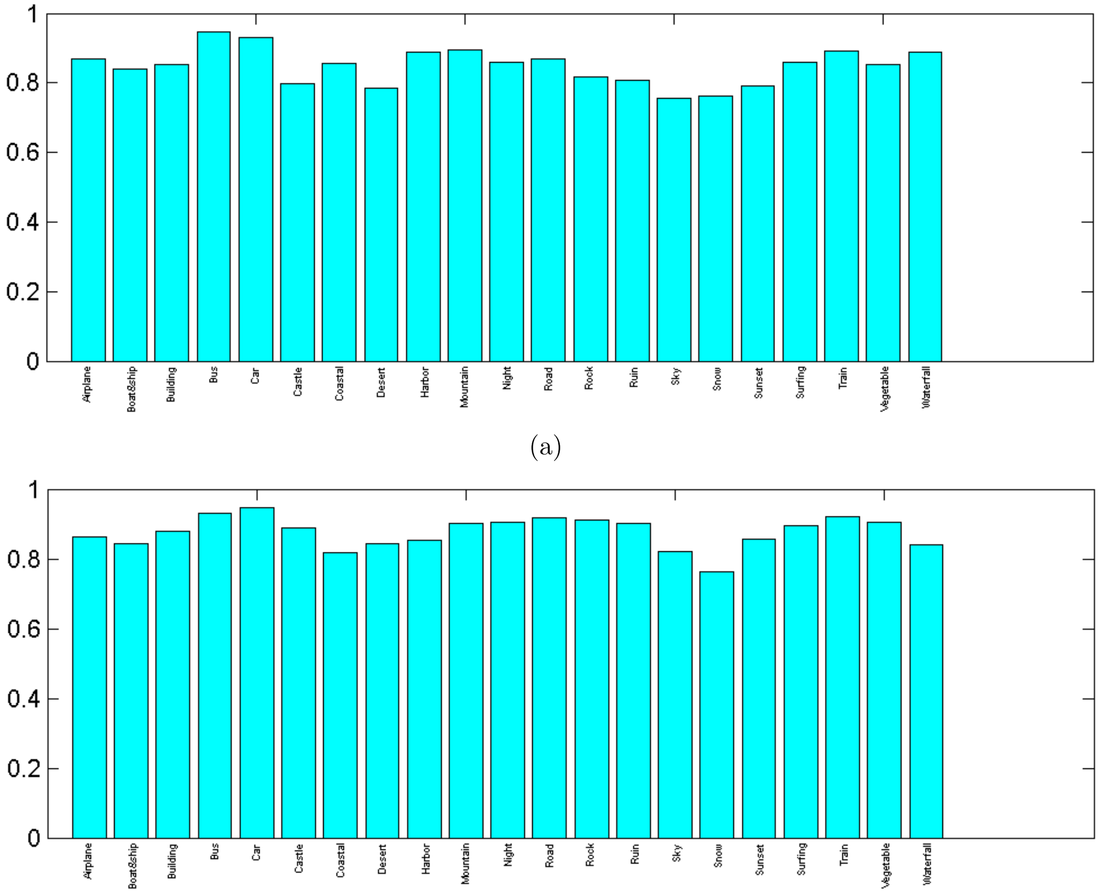

(a)

(b)

Figure 7.6: Mean average precision values (MAP) according to class posterior probabilities of each scene category of COREL dataset: (a) MAP values for the codebook that is constructed by using HSV histograms of the regions, (b) MAP values for the codebook that is constructed by using HSV and orientation histograms of the regions

illustrates the mean average precision values of each scene category again for each codebook type respectively. MAP values are calculated for the original retrieval and the following 4 iterations. For both of codebook representations the first iteration gave the largest increase in precision. A little rise is obtained for the next 4 iterations. The precision values for the codebook representation which is constructed using the combination of HSV histograms and orientation histograms is much higher than the codebook representation which is constructed using only HSV histograms. It is assumed that orientation characteristics of the lines segments in a region can be a distinguishing property for that region. On the other hand, color information in a region can be variable. For example assume that a region from a building and a region from a road. The building regions generally contain line segments with two major orientations and the road regions generally contains line segments with one major orientation. On the other hand, the color information is not distinguishing information for that types of regions since it can be vary according to the material of the object in the regions.

7.3 Comparison

We ran the bag-of-words model with probabilistic latent semantic analysis [25] on the Corel dataset and obtained 19.58% accuracy (compared to 61.35% by in Figure 7.5(a) and 34.76% by in Figure 7.5(b)). Although the proposed classification results are not very satisfactory, they are better than the popular classification approaches.

In order to verify the success of our representation model which is based on probabilities of observing different semantic scene classes in the images, we perform the same retrieval scenario on the bag of regions representations of the images. Each image is represented with the histogram of regions types it contains as before the classification process. The Figure 7.9 illustrates the precision values of the original retrieval and the following 4 iterations for Corel dataset. As seen, although there are high increases in precision values after feedback iterations, the precision values for the class probability representation is higher than the values

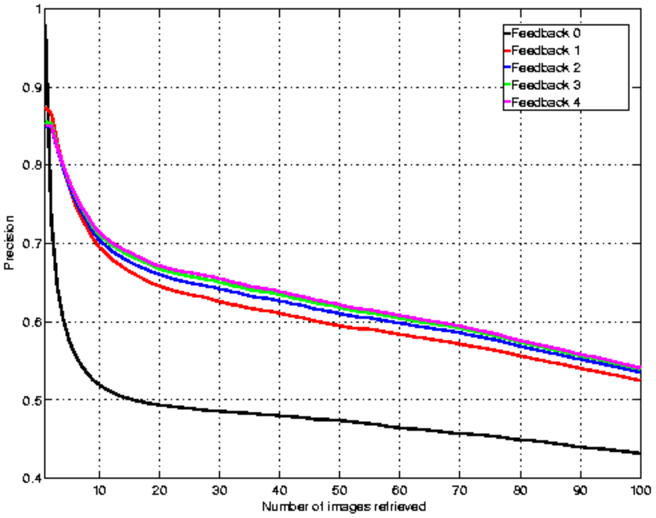

(a)

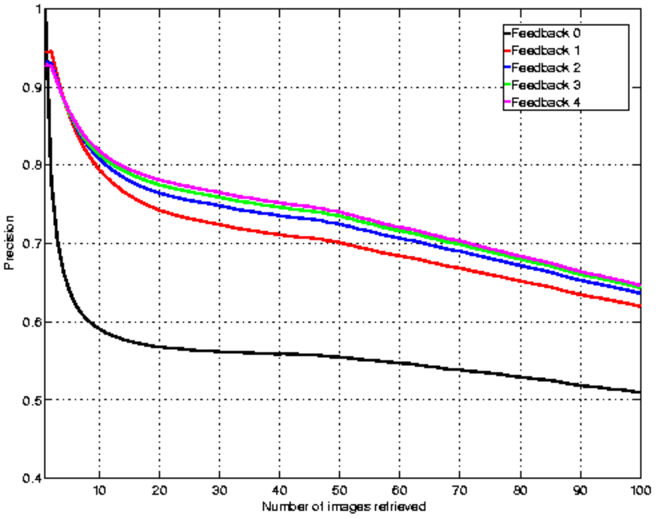

(b)

Figure 7.7: Precision vs. number of images retrieved plots of COREL for two codebook types. 'Feedback 0' refers to the retrieval without feedback: (a) Precision plot for the codebook that is constructed by using HSV histograms of the regions, (b) Precision plot for the codebook that is constructed by using HSV and orientation histograms of the regions

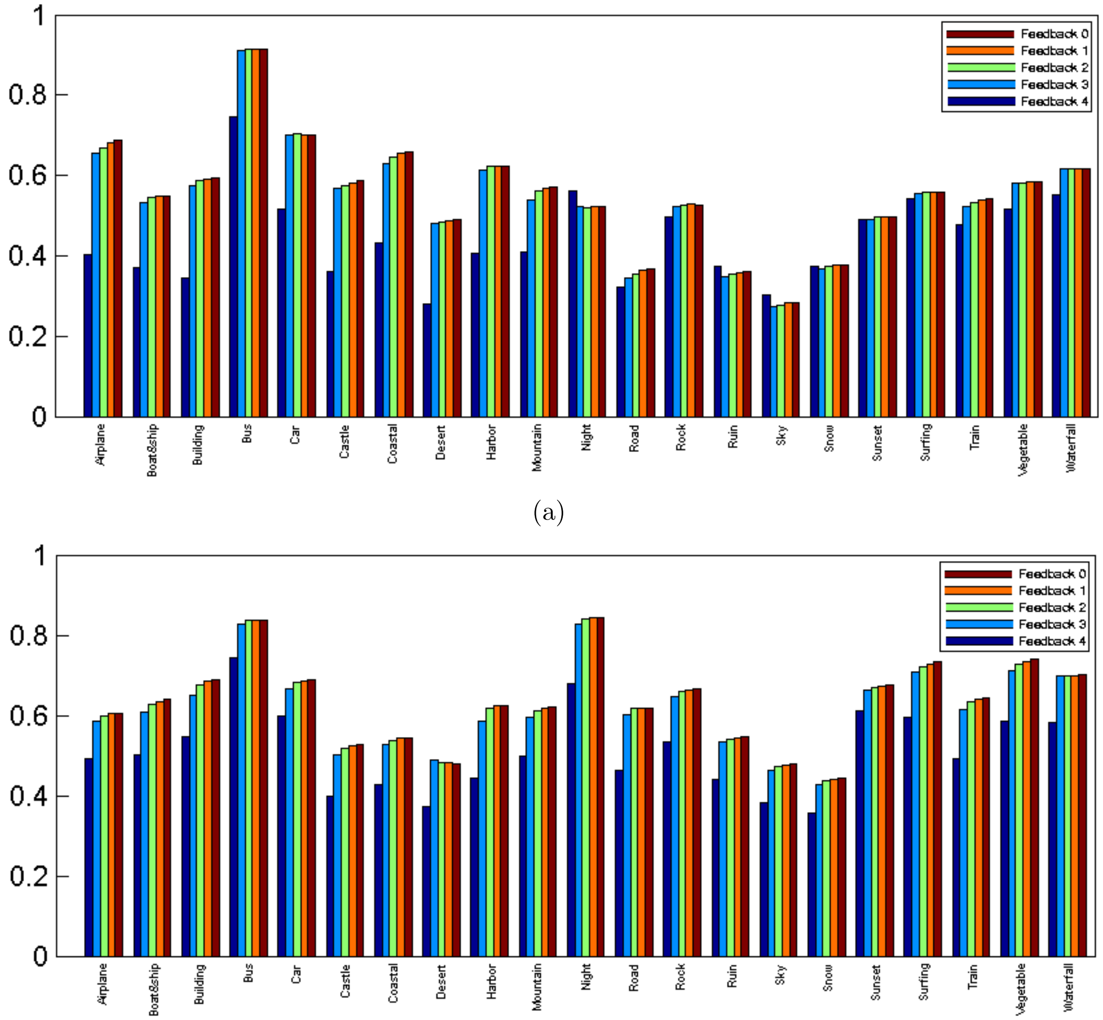

(a)

(b)

Figure 7.8: Mean average precision (MAP) graph of each scene category of COREL dataset for the original retrieval and the following 4 iterations. 'Feedback 0' refers to the retrieval without feedback: (a) MAP graph for the codebook that is constructed by using HSV histograms of the regions, (b) MAP graph for the codebook that is constructed by using HSV and orientation histograms of the regions

for the bag of regions representation.

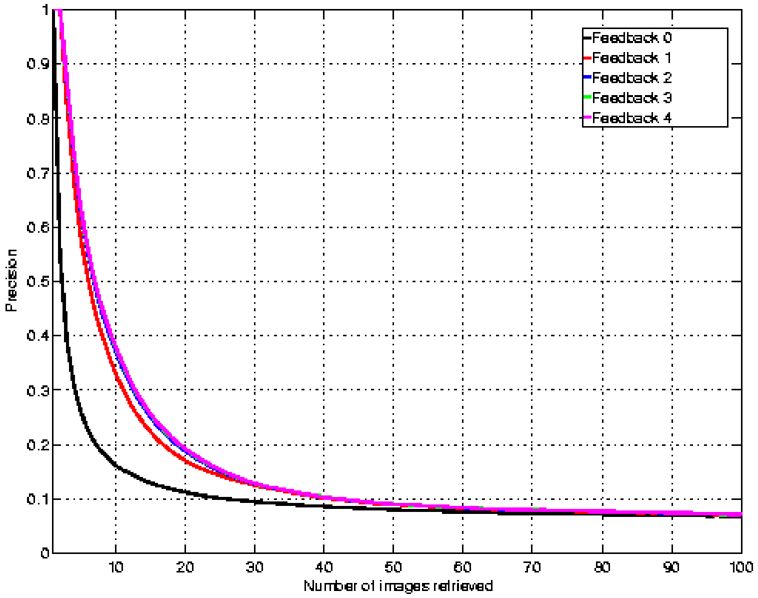

Figure 7.9: Precision vs. number of images retrieved plots of COREL for bag of regions representation

We compare our relevance feedback technique with weighted based techniques which is most preferred one to include human interaction in retrieval process because of its intuitive assumptions. Its working principle is based on assigning weights values to the low-level features and updating them according to the user feedback in CBIR.

The feedback information is incorporated into the database search in terms of iterative retrievals by modifying the contributions of different class probability values in the overall similarity computation. These modifications are done via assigning a weight to probability values of each of C classes and updating these weights in subsequent iterations. We assign a weight value $Weight_j$ to the j^{th} class. Given two images, distances d_j between their j^{th} class probability values are computed, and then, these distances are combined as the overall (dis)similarity value

$$d = \sum_{j=1}^{C} d_j * Weight_j \tag{7.1}$$

d_j is dissimilarity value between j^{th} class probability values of two images. In order to compute the weights for each class probability we use the following approach: Given the positive and negative examples for a class model being significant for a particular query the distances for the corresponding class probability values for relevant images must usually be similar (hence, a small variance), but the distances between the class probability values for relevant images and irrelevant images must usually be different (hence, a large variance). Therefore, the weights are computed using the ratio of the standard deviation of the distances between relevant and irrelevant images to the standard deviation of the distances between relevant images.

Figure 7.10 shows mean average precision values for each feedback iteration by using SVDD and Weight based approaches for (a)TRECVID and (b)Corel datasets. For TRECVID dataset we use results of the one class model and for Corel dataset we use results of the codebook that is constructed by using the combination of HSV and orientation histograms. As seen in the figures the performance of our approach is higher than the weighted approach for all feedback iterations of both datasets.

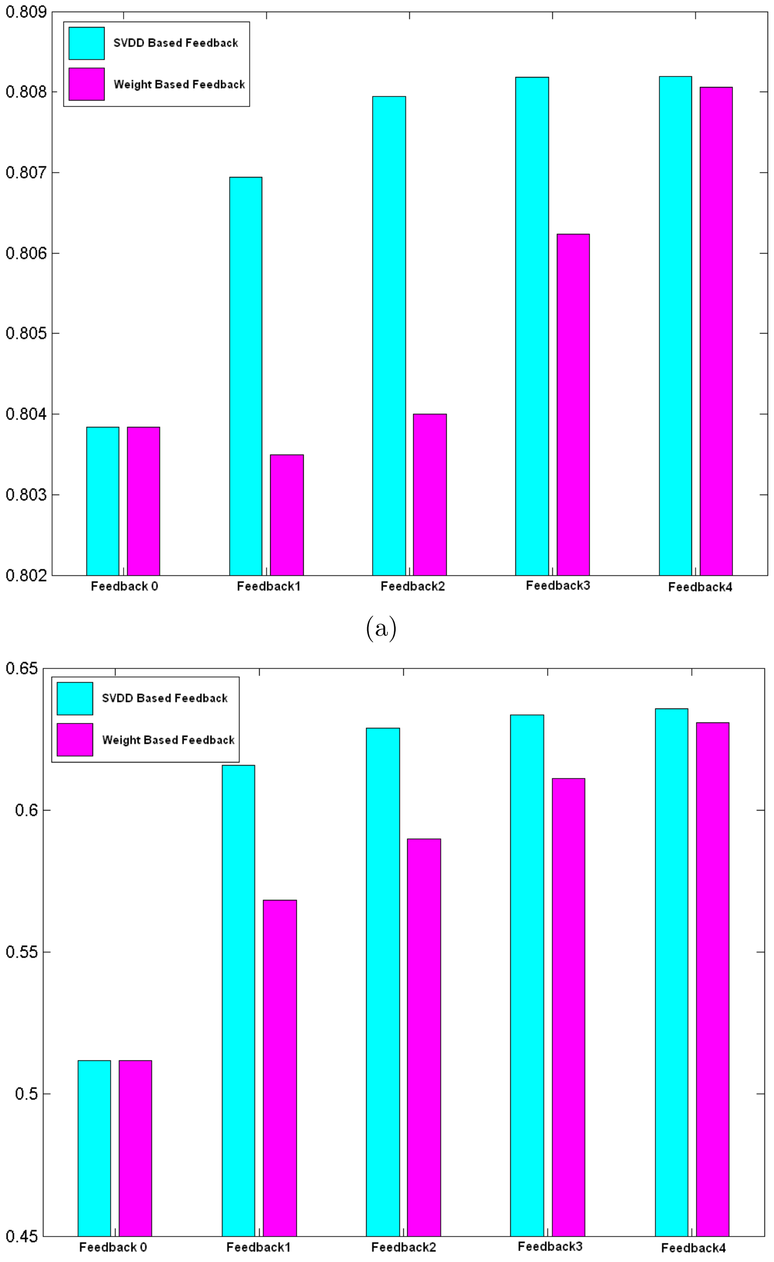

(a)

(b)

Figure 7.10: Mean average precision (MAP) graph of the original retrieval and the following 4 iterations for SVDD based and weight based feedback approaches. ‘Feedback 0’ refers to the retrieval without feedback: (a) MAP graph for TRECVID dataset, (b) MAP graph for Corel dataset

Chapter 8

CONCLUSION

In this study, a content-based image retrieval framework that is based on scene classification for image indexing is proposed. Instead of using low-level features to index the images as in traditional CBIR approaches, classification results are used to represent the images semantically. Each image is indexed with the probability of observing different semantic classes in it. To obtain the probabilities, both multi-class and one-class classification techniques are used. First, the images are segmented into meaningful regions by using two different information from the images: color and line structure. The line structure information is used for the regions that do not consist of uniform colors such as man made structures. After all regions are clustered with k-means clustering algorithm, each image is represented with the histogram of the region types it contains and the histograms are classified by using Bayesian framework. For probability estimation two different models are used: multi class and one class. In the multi class model, the region types are treated independently and class-condition probabilities are estimated using multinomial model. This model is not suitable for TRECVID dataset since the classes are not mutually exclusive. Therefore, in addition to multi class model, one class model is used. In one class modeling Gaussian classifier in each class is trained independently and probability density function is estimated for the training set of each class. The classification results are not satisfactory since assigning the images to the class with the highest probability is not suitable in a dataset which contains classes that overlap semantically. These results show that associating the images with a single class with the highest probability is not sufficient in retrieval process. Therefore, images are represented with the posterior class probability values that come from classification process. In order to minimize the semantic gap between the image similarity understanding of humans and the computer one class support vector data description based relevance feedback is performed. The performance of retrieval process based on one class classification is higher than multi class classification for TRECVID dataset since the semantical class overlapping is very high in this dataset. Both in TRECVID and Corel datasets the results are very satisfactory. We compare our results with a weight based relevance feedback technique. The comparison results show that the performance of our approach is much higher.

Bibliography

[1] J. Canny. A computational approach to edge detection. *IEEE Transactions on Pattern Analysis and Machine Intelligence*, 8(6):679–698, 1986.

[2] Gustavo Carneiro, Antoni B. Chan, and Pedro J. Moreno. Supervised learning of semantic classes for image annotation and retrieval. *IEEE Transactions on Pattern Analysis and Machine Intelligence*, 29(3):394–410, 2007.

[3] Yunqiang Chen, Xiang Sean Zhou, and T.S. Huang. One-class svm for learning in image retrieval. In *International Conference on Image Processing - Volume 1*, pages 34–37, 2001.

[4] Ingemar J. Cox, Matt L. Miller, Thomas P. Minka, Thomas V. Papathomas, and Peter N. Yianilos. The bayesian image retrieval system, pichunter: theory, implementation, and psychophysical experiments. *IEEE Transactions on Image Processing*, 2000.

[5] A. Etemadi. Robust segmentation of edge data. In *International Conference on Image Processing and its Applications*, pages 311–314, 1992.

[6] G. Giacinto and F. Roli. Bayesian relevance feedback for content-based image retrieval. *Pattern Recognition*, 37(7):1499–1508, 2004.

[7] M.M. Gorkani and R.W. Picard. Texture orientation for sorting photos at a glance. In *Proceedings of the 12th IAPR International Conference on Pattern Recognition - Volume 1*, pages 459–464, 1994.

[8] Guo-Dong Guo, A.K. Jain, Wei-Ying Ma, and Hong-Jiang Zhang. Learning similarity measure for natural image retrieval with relevance feedback. *IEEE Transactions on Neural Networks*, 13(4):811–820, 2002.

[9] Jing Huang, S. Ravi Kumar, Mandar Mitra, Wei-Jing Zhu, and Ramin Zabih. Image indexing using color correlograms. In *Proceedings of the 1997 Conference on Computer Vision and Pattern Recognition (CVPR)*, page 762, 1997.

[10] Feng Jing, Mingjing Li, Lei Zhang, Hong jiang Zhang, and Bo Zhang. Learning in region-based image retrieval. In *Proceedings of the IEEE International Symposium on Circuits and Systems*, pages 206–215, 2003.

[11] Carmen Lai, David M. J. Tax, Robert P. W. Duin, Elzbieta Pekalska, and Pavel Paclík. On combining one-class classifiers for image database retrieval. In *Proceedings of the Third International Workshop on Multiple Classifier Systems (MCS)*, pages 212–221, 2002.

[12] Svetlana Lazebnik, Cordelia Schmid, and Jean Ponce. Beyond bags of features: Spatial pyramid matching for recognizing natural scene categories. In *Proceedings of the 2006 IEEE Computer Society Conference on Computer Vision and Pattern Recognition (CVPR)*, pages 2169–2178, 2006.

[13] Zhang Lei, Lin Fuzong, and Zhang Bo. A cbir method based on color-spatial feature. In *Proceedings of the IEEE Region 10 Conference (TENCON 99.) - Volume 1*, pages 166–169, 1999.

[14] Fei-Fei Li and Pietro Perona. A bayesian hierarchical model for learning natural scene categories. In *Proceedings of the 2005 IEEE Computer Society Conference on Computer Vision and Pattern Recognition (CVPR) - Volume 2*, pages 524–531, 2005.

[15] Yi Li and Linda G. Shapiro. Consistent line clusters for building recognition in cbir. In *Proceedings of the 16 th International Conference on Pattern Recognition (ICPR) - Volume 3*, page 30952, 2002.

[16] Yi Li, Linda G. Shapiro, and Jeff A. Bilmes. A generative/discriminative learning algorithm for image classification. In *Proceedings of the Tenth IEEE International Conference on Computer Vision (ICCV)*, pages 1605–1612, 2005.

[17] Marcin Marszaek and Cordelia Schmid. Spatial weighting for bag-of-features. In *Proceedings of the 2006 IEEE Computer Society Conference on Computer Vision and Pattern Recognition (CVPR)*, pages 2118–2125, 2006.

[18] Krystian Mikolajczyk, Bastian Leibe, and Bernt Schiele. Local features for object class recognition. In *Proceedings of the Tenth IEEE International Conference on Computer Vision (ICCV)*, pages 1792–1799, 2005.

[19] R. Mojena. ierarchical grouping methods and stopping rules: An evaluation. *The Computer Journal*, 20(4):359–363, 1977.

[20] Florent Monay, Pedro Quelhas, Jean-Marc Odobez, and Daniel Gatica-Perez. Integrating co-occurrence and spatial contexts on patchbased scene segmentation. In *Proceedings of the 2006 Conference on Computer Vision and Pattern Recognition Workshop (CVPRW)*, page 14, 2006.

[21] Takashi Onoda, Hiroshi Murata, and Seiji Yamada. One class classification methods based non-relevance feedback document retrieval. In *Proceedings of the 2006 IEEE/WIC/ACM international conference on Web Intelligence and Intelligent Agent Technology (WI-IATW)*, pages 393–396, 2006.

[22] Paclk Pavel, Robert P. W. Duin, Geert M. P. Van Kempen, and R. Kohlus. Segmentation of multi-spectral images using the combined classifier approach. *Image and Vision Computing*, 21(6):473–482, 2003.

[23] Jing Peng, Bir Bhanu, and Shan Qing. Probabilistic feature relevance learning for content-based image retrieval. *Computer Vision and Image Understanding*, 75(1-2):150–164, 1999.

[24] P. Quelhas, F. Monay, J.-M. Odobez, D. Gatica-Perez, T. Tuytelaars, and L. Van Gool. Modeling scenes with local descriptors and latent aspects. In *Proceedings of the Tenth IEEE International Conference on Computer Vision (ICCV) - Volume 1*, pages 883–890, 2005.

[25] Pedro Quelhas, F. Monay, J.-M. Odobez, D. Gatica-Perez, and T. Tuytelaars. A thousand words in a scene. *IEEE Transactions on Pattern Analysis and Machine Intelligence*, 29(9):1575–1589, 2007.

[26] Yong Rui, T.S. Huang, M. Ortega, and S. Mehrotra. Relevance feedback: a power tool for interactive content-based image retrieval. *IEEE Transactions on Circuits and Systems for Video Technology*, 8(5):644–655, 1998.

[27] Cordelia Schmid and Roger Mohr. Local grayvalue invariants for image retrieval. *IEEE Transactions on Pattern Analysis and Machine Intelligence*, 19(5):530–535, 1997.

[28] L. Setia, J. Ick, and H. Burkhardt. Svm-based relevance feedback in image retrieval using invariant feature histograms. In *Proceedings of the IAPR Workshop on Machine Vision Applications*, pages 136–139, 2005.

[29] John R. Smith and Chung-Sheng Li. Image classification and querying using composite region templates. *Computer Vision and Image Understanding*, 75(1-2):165–174, 1999.

[30] Markus A. Stricker and Markus Orengo. Similarity of color images. In *Storage and Retrieval for Image and Video Databases (SPIE)*, pages 381–392, 1995.

[31] Martin Szummer and Rosalind W. Picard. Indoor-outdoor image classification. In *Proceedings of the 1998 International Workshop on Content-Based Access of Image and Video Databases (CAIVD)*, page 42, 1998.

[32] David M. J. Tax and Robert P. W. Duin. Support vector data description. *Machine Learning*, 54(1):45–66, 2004.

[33] A. Vailaya, M.A.T. Figueiredo, A.K. Jain, and Hong-Jiang Zhang. Image classification for content-based indexing. *IEEE Transactions on Image Processing*, 10(1):117–130, 2001.

[34] A. Vailaya, A. Jain, and H. J. Zhang. On image classification: City vs. landscape. In *Proceedings of the IEEE Workshop on Content - Based Access of Image and Video Libraries (CBAIVL)*, page 3, 1998.

[35] Jan C. van Gemert, Jan-Mark Geusebroek, Cor J. Veenman, Cees G. M. Snoek, and Arnold W. M. Smeulders. Robust scene categorization by learning image statistics in context. In *CVPRW '06: Proceedings of the 2006 Conference on Computer Vision and Pattern Recognition Workshop (CVPRW)*, page 105, 2006.

[36] N. Vasconcelos. On the efficient evaluation of probabilistic similarity functions for image retrieval. *IEEE Transactions on Information Theory*, 50(7):1482–1496, 2004.

[37] Julia Vogel and Bernt Schiele. Semantic modeling of natural scenes for content-based image retrieval. *International Journal of Computer Vision*, 72(2):133–157, 2007.

[38] James Ze Wang, Jia Li, and Gio Wiederhold. Simplicity: Semantics-sensitive integrated matching for picture libraries. In *Proceedings of the 4th International Conference on Advances in Visual Information Systems (VISUAL)*, pages 360–371, 2000.

[39] Rong Yan, Apostol Natsev, and Murray Campbell. An efficient manual image annotation approach based on tagging and browsing. In *Workshop on multimedia information retrieval on The many faces of multimedia semantics (MS)*, pages 13–20, 2007.

[40] Xiang Sean Zhou and Thomas S. Huang. Relevance feedback in content-based image retrieval: some recent advances. *Information Sciences*, 148(1-4):129–137, 2002.

Appendix A

Support Vector Data Description

(Taken from [32])

A.1 Normal data description

Assume that $\mathbf{x}$ is a column vector and we want to find a description for a dataset that contains N data objects $\{\mathbf{x}_i, i = 1, \ldots, N\}$. The data description models a closed boundary which is a hypersphere with minimum radius that contains all data points. Error function is defined to minimize the volume of hypersphere:

$$F(R, \mathbf{a}) = R^2 \tag{A.1}$$

with constraints:

$$\|\mathbf{x}_i - \mathbf{a}\|^2 \leq R^2, \forall i \tag{A.2}$$

If the hypersphere is enlarged in order to force to obtain all data points with outliers, the hypersphere with a large radius will not represent the data very well. Therefore, some data points are allowed to be outside of the sphere and they are called slack variables. Minimization problem changes into:

$$F(R, \mathbf{a}) = R^2 + C \sum_i \xi_i \tag{A.3}$$

with constraints

$$\|\mathbf{x}_i - \mathbf{a}\|^2 \leq R^2 + \xi_i, \xi_i \geq 0 \forall i \tag{A.4}$$

where the parameter C gives the trade-off between the volume and the errors.

Incorporate Eq. A.3 into Eq. A.4 with Lagrange multipliers following equation is obtained:

$$\begin{aligned} L(R, \mathbf{a}, \alpha_i, \gamma_i, \xi_i) &= R^2 + C \sum_i \xi_i + \sum_i \alpha_i \{R^2 + \xi_i - (\|\mathbf{x}_i\|^2 - 2\mathbf{a}.\mathbf{x}_i + \|\mathbf{a}\|^2)\} \\ &- \sum_i \gamma_i \xi_i \end{aligned} \tag{A.5}$$

with the Lagrange multipliers $\alpha_i \geq 0$ and $\gamma_i \geq 0$. L should be minimized with respect to R, $\mathbf{a}$, ξ_i and maximized with respect to α_i and γ_i .

Setting partial derivatives to zero gives the constraints:

$$\frac{\partial L}{\partial R} = 0 : \sum_i \alpha_i = 1 \tag{A.6}$$

$$\frac{\partial L}{\partial \mathbf{a}} = 0 : \mathbf{a} = \frac{\sum_i \alpha_i \mathbf{x}_i}{\sum_i \alpha_i} = \sum_i \alpha_i \mathbf{x}_i \tag{A.7}$$

$$\frac{\partial L}{\partial \xi_i} = 0 : C - \alpha_i - \gamma_i = 0 \tag{A.8}$$

when we demand $0 \leq \alpha_i \leq C$ we can remove the variables γ_i from the Eq. A.5 since $\alpha_i \geq 0$, $\gamma_i \geq 0$.

Resubstituting Eq. A.6 Eq. A.8 into Eq. A.5 results in:

$$L = \sum_i \alpha_i (\mathbf{x}_i \mathbf{x}_i) - \sum_{i,j} \alpha_i \alpha_j (\mathbf{x}_i \mathbf{x}_j) \tag{A.9}$$

with constraints

$$0 \le \alpha_i \le C \tag{A.10}$$

Maximizing Eq. A.9 gives a set α_i. Lagrange multiplier α_i will be zero when the inequality $\|\mathbf{x}_i - \mathbf{a}\|^2 < R^2 + \xi_i$ is satisfied by $\mathbf{x}_i$ and α_i become bigger than zero when the equality $\|\mathbf{x}_i - \mathbf{a}\|^2 = R^2 + \xi_i$ is satisfied by $\mathbf{x}_i$.

$$\|\mathbf{x}_i - \mathbf{a}\|^2 < R^2 \rightarrow \alpha_i = 0, \gamma_i = 0 \tag{A.11}$$

$$\|\mathbf{x}_i - \mathbf{a}\|^2 = R^2 \rightarrow 0 < \alpha_i < C, \gamma_i = 0 \tag{A.12}$$

$$\|\mathbf{x}_i - \mathbf{a}\|^2 > R^2 \rightarrow \alpha_i = C, \gamma_i > 0 \tag{A.13}$$

The objects $\mathbf{x}_i$ with $\alpha_i > 0$ will be called support vectors. An object $\mathbf{z}$ is accepted if the distance of the object to the center of the sphere is smaller than or equal to the radius

$$\|\mathbf{z} - \mathbf{a}\|^2 = (\mathbf{z}.\mathbf{z}) - 2\sum_i \alpha_i(\mathbf{z}.\mathbf{x}_i) + \sum_{i,j} \alpha_i\alpha_j(\mathbf{x}_i.\mathbf{x}_j) \le R^2 \tag{A.14}$$

where R^2 is the distance from the center of the sphere $\mathbf{a}$ to (any of the support vector on) the boundary. Support Vectors which fall outside the description are excluded. Therefore:

$$R^2 = (\mathbf{x}_s.\mathbf{x}_s) - 2\sum_i \alpha_i(\mathbf{x}_i.\mathbf{x}_s) + \sum_{i,j} \alpha_i\alpha_j(\mathbf{x}_i.\mathbf{x}_j) \tag{A.15}$$

for any support vector $\mathbf{x}_s$ which have $\alpha_s < C$.

A.2 SVDD with negative examples

Assume again we want to find a description for a dataset that contains N data objects $\{\mathbf{x}_i, i = 1, \ldots, N\}$. However this time we have M negative data objects

$\{\mathbf{x}_l, l = N+1, \ldots, N+M\}$ that we do not want them to be inside the hypersphere which contains the target data objects. Two types of slack variables, ξ_i and ξ_l are introduced this time to allow outliers from the target set and from the negative set and the error function becomes:

$$F(R, \mathbf{a}, \xi_i, \xi_l) = R^2 + C_1 \sum_i \xi_i + C_2 \sum_l \xi_l \tag{A.16}$$

with constraints:

$$\|\mathbf{x}_i - \mathbf{a}\|^2 \leq R^2 + \xi_i, \|\mathbf{x}_l - \mathbf{a}\|^2 \geq R^2 + \xi_l, \xi_i \geq 0, \xi_l \geq 0, \forall i, l \tag{A.17}$$

These constraints are again incorporated in Eq. A.16 by using the Lagrange multipliers α_i, α_l, γ_i and γ_l, which are all bigger than 0.

$$\begin{aligned} L(R, \mathbf{a}, \xi_i, \xi_l, \alpha_i, \alpha_l, \gamma_i, \gamma_l) &= R^2 + C_1 \sum_i \xi_i + C_2 \sum_l \xi_l \\ &- \sum_i \alpha_i \{R^2 + \xi_i - (\|\mathbf{x}_i\|^2 - 2\mathbf{a}.\mathbf{x}_i + \|\mathbf{a}\|^2)\} \\ &- \sum_l \alpha_l \{R^2 + \xi_l - (\|\mathbf{x}_l\|^2 - 2\mathbf{a}.\mathbf{x}_l + \|\mathbf{a}\|^2)\} \\ &- \sum_i \gamma_i \xi_i - \sum_l \gamma_l \xi_l \end{aligned} \tag{A.18}$$

After setting the partial derivatives of L with respect to R, $\mathbf{a}$, ξ_i and ξ_l to zero we get the constraints:

$$\sum_i \alpha_i - \sum_l \alpha_l = 1 \tag{A.19}$$

$$\mathbf{a} = \sum_i \alpha_i \mathbf{x}_i - \sum_l \alpha_l \mathbf{x}_l \tag{A.20}$$

$$0 \leq \alpha_i \leq C_1, 0 \leq \alpha_l \leq C_2, \forall i, l \tag{A.21}$$

Resubstituting Eq. A.19 - Eq. A.21 into Eq. A.18 results in:

$$\begin{aligned} L &= \sum_i \alpha_i(\mathbf{x}_i\mathbf{x}_i) - \sum_l \alpha_l(\mathbf{x}_l\mathbf{x}_l) - \sum_{i,j} \alpha_i\alpha_j(\mathbf{x}_i\mathbf{x}_j) \\ &+ 2\sum_{l,j} \alpha_l\alpha_j(\mathbf{x}_l\mathbf{x}_j) - \sum_{l,m} \alpha_l\alpha_m(\mathbf{x}_l\mathbf{x}_m) \end{aligned}$$

(A.22)

If we introduce a new variable $\alpha'_k = y_k\alpha_k$, where $k = 1, \ldots, N + M$ and y_k is 1 for target data and -1 for negative data, Eq. A.19 becomes $\sum_k \alpha'_k = 1$ and Eq. A.20 becomes $\mathbf{a} = \sum_k \alpha'_k\mathbf{x}_k$. We can again use the testing function Eq. A.14. Therefore if the negative data objects are available with the target data, Eq. A.9 is replaced with Eq. A.22 and $\alpha'_k$is used instead of α_i.